Available online at www.sciencedirect.com
SCIENCE DIRECT®
Applied Numerical Mathematics 56 (2006) 814–843
APPLIED NUMERICAL MATHEMATICS
www.elsevier.com/locate/apnum

Globally conservative properties and error estimation of a multi-symplectic scheme for Schrödinger equations with variable coefficients ☆

Jialin Hong [a,*], Ying Liu [b], Hans Munthe-Kaas [c], Antonella Zanna [c]

[a] *State Key Laboratory of Scientific and Engineering Computing, Institute of Computational Mathematics and Scientific/Engineering Computing, Academy of Mathematics and System Sciences, Chinese Academy of Sciences, PO Box 2719, Beijing 100080, PR China*

[b] *Department of Mathematical Sciences, Tsinghua University, Beijing 100084, PR China*

[c] *Institutt for Informatikk, N-5020 Bergen, Norway*

Abstract

Based on the multi-symplecticity of the Schrödinger equations with variable coefficients, we give a multi-symplectic numerical scheme, and investigate some conservative properties and error estimation of it. We show that the scheme satisfies discrete normal conservation law corresponding to one possessed by the original equation, and propose global energy transit formulae in temporal direction. We also discuss some discrete properties corresponding to energy conservation laws of the original equations. In numerical experiments, the comparisons with modified Goldberg scheme and Modified Crank–Nicolson scheme are given to illustrate some properties of the multi-symplectic scheme in the numerical implementation, and the global energy transit is monitored due to the scheme does not preserve energy conservation law. Our numerical experiments show the match between theoretical and corresponding numerical results.

Keywords: Schrödinger equations; Conservation laws; Error estimation; Global energy transit; Multi-symplectic integrators

☆ This work is supported by the Director Innovation Foundation of ICMSEC and AMSS, the Foundation of CAS, the NNSFC (No. 19971089) and the Special Funds for Major State Basic Research Projects of China G1999032804.

* Corresponding author.
E-mail address: hjl@lsec.cc.ac.cn (J. Hong).

0168-9274/$30.00 © 2005 IMACS. Published by Elsevier B.V. All rights reserved.
doi:10.1016/j.apnum.2005.06.006

1. Introduction

In the last two decades, symplectic schemes for finite-dimensional Hamiltonian systems are proven to be more accurate and efficient than non-symplectic schemes for long-time numerical computations and are nowadays applied to a number of practical problems arising in many fields of science and engineering which involve celestial mechanics, quantum physics, statistics and so on (see [6,10,12,15,20–22,24,32, 33,36,38,42] and references therein).

If nowadays symplecticity for finite-dimensional Hamiltonians is reasonably well understood, it is only in the last few years that researchers have started investigating the case of Hamiltonian PDEs. For infinite-dimensional systems one has the choice between symplecticity and multi-symplecticity, the first being a global property, the second local. However, under appropriate circumstances, it is possible to show that the local preservation of multi-symplecticity can be used to preserve global properties of the PDE under consideration.

For the theoretical background on multi-symplecticity for Hamiltonian PDEs with constant coefficients we refer the reader to [4,5,8,18,21,29–31,37] and references therein.

Multi-symplecticity preserving numerical methods for Hamiltonian PDEs have displayed much better numerical behavior for long-time computations too. For instance, in [5] the authors show that their multi-symplectic integrator, based on the central box discretization, has remarkable energy and momentum conservation; moreover when the function $S(z)$ (in Eq. (15)) in the multi-symplectic formula of Hamiltonian PDEs is quadratic in z, the multi-symplectic box scheme conserves discrete local energy and local momentum exactly.

In the numerical experiments in [21] both the local and global conservation of energy and momentum are monitored and it is found that the global momentum and norm are preserved within roundoff [21, p. 125]. And it is substantiated numerically that the global conservation properties are weaker conditions (also see [37]). It is well known that Hamiltonian PDEs with variable coefficients also have some concrete global conservation laws. Typical examples are normalization for the time-dependent linear Schrödinger equation in quantum physics (see [11,13,25,26,34,35,44]) and energy/momentum for the nonlinear Schrödinger equation with variable coefficients arising in optics and other applications. Thus we are motivated to investigate the globally conservative properties of multi-symplectic structure-preserving discretizations of Hamiltonian PDEs with variable coefficients. We refer to [23,27,28,39,41, 45] and references therein for further reading about discrete global conservation laws for a family of finite-difference schemes. In this paper we focus mainly on globally conservative properties, and their application to error estimate, of the multi-symplectic scheme for nonlinear variable-coefficient Schrödinger equations. Multi-symplectic methods for a variety of other Hamiltonian PDEs with variable coefficients arising from applications are presented in [16,17].

We consider the one-dimensional Cauchy problem

$$\begin{aligned} &\mathrm{i}\psi_t + \alpha(t)\psi_{xx} + \Psi'_{|\psi|^2}\big(|\psi|^2, x, t\big)\psi = 0, \\ &\psi(x,0) = \varphi(x), \end{aligned} \tag{1}$$

where $\alpha(t)$ ($\alpha(t) \not\equiv 0$) is a bounded real function of $t \in \mathbb{R}$ ($\alpha(t) \equiv 0$ is an interesting case, it will be discussed in another paper), and $\Phi(\psi, x, t) = \Psi(|\psi|^2, x, t)$ is a real differentiable function of $(\psi, x, t) \in$

$\mathbb{C} \times \mathbb{R} \times \mathbb{R}$, such that $\Psi''_{|\psi|^2}(|\psi|^2, x, t)$ is a bounded function of x and t for every $\psi \in \mathbb{C}$. As usual, $\mathrm{i} = \sqrt{-1}$, and, moreover, $\varphi(x)$ is a smooth function such that

$$E_1(\varphi) = \int_{\mathbb{R}} \left|\varphi(x)\right|^2 dx < +\infty, \tag{2}$$

(the so-called *L_2-function*).

The theoretical investigation of problem (1) can be found in [3,44] and references therein. Throughout the paper we assume that the solution ψ of (1) exists globally and satisfies $\lim_{|x|\to+\infty}(|\psi| + |\psi_x|) = 0$.

Before proceeding further, we derive three global conservation laws (norm, momentum and energy) for (1). The first is done by multiplying (1) by $\bar{\psi}$ and taking the imaginary part, and multiplying (1) by $\bar{\psi}_t$ and then taking the real part. The next two can be obtained by a similar way.

Proposition 1. *Under our assumptions, the solution ψ of the problem* (1) *satisfies*

(1) $E_1(\psi) = \int_{\mathbb{R}} |\psi|^2 dx = E_1(\varphi)$ (*global norm conservation*);
(2) $M(\psi) = \int_{\mathbb{R}} (\Re(\psi)\Im(\psi_x) - \Re(\psi_x)\Im(\psi))\, dx = M(\varphi)$ (*global momentum conservation*);
(3) *if Ψ is independent of t and $\alpha(t) \equiv$ constant, then*

$$E_2(\psi) = \int_{\mathbb{R}} \left(\alpha|\psi_x|^2 - \Psi\left(|\psi|^2, x\right)\right) dx = E_2(\varphi), \tag{3}$$

where φ is the initial function in (1) *and satisfies*

$$E_2(\varphi) = \int_{\mathbb{R}} \left(\alpha|\varphi_x|^2 - \Psi\left(|\varphi|^2, x\right)\right) dx < +\infty.$$

(3) *stands for global energy conservation.*

Obviously, if Ψ is dependent on t, then (1), in general, does not have the property of global energy conservation. Because the study of global momentum conservation is quite similar to that of global norm conservation, we will omit some details of discrete global momentum conservation of multi-symplectic integrators.

In order to investigate the numerical behavior of the solution of (1) under numerical discretization, we introduce a uniform grid $(x_j, t_k) \in \mathbb{R}^2$ with mesh-size Δt in the t direction and mesh-size Δx in the x-direction. The value of the function $\psi(x, t)$ at the mesh point (x_j, t_k) is denoted by $\psi_{j,k}$. Furthermore, we will denote

$$\psi_{j-\frac{1}{2},k} := \frac{1}{2}(\psi_{j,k} + \psi_{j-1,k}), \qquad \psi_{j,k-\frac{1}{2}} := \frac{1}{2}(\psi_{j,k} + \psi_{j,k-1}),$$

and

$$\|\psi_k\|^2 := \Delta x \sum_j |\psi_{j,k}|^2, \qquad \|\psi_k\|^2_{\frac{1}{2}} := \Delta x \sum_j |\psi_{j-\frac{1}{2},k}|^2$$

(we assume that the two last sums are finite).

A numerical scheme for problem (1) can be constructed as follows

$$\frac{\mathrm{i}}{\Delta t}(\psi_{j,k+1}-\psi_{j,k})+\frac{\alpha(t_{k+\frac{1}{2}})}{2\Delta x^2}\big((\psi_{j+1,k+1}-2\psi_{j,k+1}+\psi_{j-1,k+1})+(\psi_{j+1,k}-2\psi_{j,k}+\psi_{j-1,k})\big)$$
$$+\frac{\Psi(|\psi_{j,k+1}|^2,x_j,t_{k+\frac{1}{2}})-\Psi(|\psi_{j,k}|^2,x_j,t_{k+\frac{1}{2}})}{2(|\psi_{j,k+1}|^2-|\psi_{j,k}|^2)}(\psi_{j,k+1}+\psi_{j,k})=0 \tag{4}$$

(*modified Crank–Nicolson scheme*), which is not a new numerical scheme and has been presented in [9] for the case of constant coefficients.

In Section 3 we will prove that this scheme possesses some conservative properties which imply convergence and stability. The discretization of gradient in nonlinear term results in nonmulti-symplecticity of the scheme.

The present paper is organized as follows: in the rest of this section we recall some globally classical conservation laws and well-known numerical schemes for the time-dependent Schrödinger equations in quantum physics and nonlinear Schrödinger equations with variable coefficients.

A multi-symplectic scheme for the Schrödinger equations with variable coefficients is introduced in Section 2. In Section 3 we discuss the globally conservative properties of the multi-symplectic scheme. The scheme satisfies a discrete analogue of the classically global conservation laws mentioned in previous sections. The global energy transit formulae in temporal direction are presented. The error of the proposed multi-symplectic scheme then is estimated in Section 4 by means of numerically global conservation laws. Section 5 is divided into two parts. In the first part we present some numerical experiments to compare the numerical behavior of the multi-symplectic scheme proposed in Section 2 with other two schemes. In the last part of Section 5 we monitor the global energy transit under the multi-symplectic scheme.

1.1. The time-dependent Schrödinger equation in quantum physics

Substituting $\alpha(t)=\frac{\hbar}{2m}$ and $\Psi'_{|\psi|^2}(|\psi|^2,x,t)=-\frac{1}{\hbar}V(x,t)$ in (1) yields

$$\begin{aligned}&\mathrm{i}\hbar\psi_t+\frac{\hbar^2}{2m}\psi_{xx}+V(x,t)\psi=0,\\&\psi(x,0)=\varphi(x),\end{aligned} \tag{5}$$

where $V(x,t)$ is a bounded real function, the potential, m is the mass of the particle, ψ is the wave-function and finally $h=2\pi\hbar$ is Planck's constant. The linear problem (5) is a fundamental equation in quantum physics [11–13,19,25,26,34,39]. It describes the propagation of a quantum particle, for instance an electron, in a potential field given by V (e.g., the usual Coulomb potential for the hydrogen atom). The square of the wave-function, ψ^2, describes the probability distribution for the position of the particle. In this case, the first item and third item in Proposition 1 can be rewritten as

Proposition 2.

(1) $$E_1(\psi)=\int_{\mathbb{R}}\big|\psi(x,t)\big|^2\,dx=E_1(\varphi). \tag{6}$$

(2) *If V is independent of t, then*

$$E_2(\psi) = \int_{\mathbb{R}} \left(\frac{\hbar}{2m} \left|\psi_x(x,t)\right|^2 - \frac{V(x)}{\hbar} \left|\psi(x,t)\right|^2 \right) dx = E_2(\varphi), \tag{7}$$

where $E_2(\varphi) = \int_{\mathbb{R}} (\frac{\hbar}{2m}|\varphi'|^2 - \frac{V(x)}{\hbar}|\varphi|^2)\, dx$.

When V is independent of t, a famous scheme for (5) in quantum physics is

$$\frac{\mathrm{i}\hbar}{\Delta t}(\psi_{j,k+1} - \psi_{j,k}) + \frac{\hbar^2}{2m\Delta x^2}(\psi_{j+1,k+\frac{1}{2}} - 2\psi_{j,k+\frac{1}{2}} + \psi_{j-1,k+\frac{1}{2}}) + V(x_j)\psi_{j,k+\frac{1}{2}} = 0 \tag{8}$$

known as *Goldberg's scheme* [13]. The Goldberg scheme is a special case of the modified Crank–Nicolson scheme

$$\frac{\mathrm{i}\hbar}{\Delta t}(\psi_{j,k+1} - \psi_{j,k}) + \frac{\hbar^2}{2m\Delta x^2}(\psi_{j+1,k+\frac{1}{2}} - 2\psi_{j,k+\frac{1}{2}} + \psi_{j-1,k+\frac{1}{2}}) + V(x_j, t_{k+\frac{1}{2}})\psi_{j,k+\frac{1}{2}} = 0 \tag{9}$$

because of the independence of V on t.

Researchers use (8) and (9) to simulate numerically quantum states of (5). Recently, some further investigation on higher-order numerical schemes for (5) has been done in [2,19,34,35] and references therein.

1.2. Nonlinear Schrödinger equations with variable coefficients

The following nonlinear problem

$$\begin{aligned} &\mathrm{i}\psi_t + \alpha(t)\psi_{xx} + \beta(x,t)|\psi|^{p-1}\psi = 0, \\ &\psi(x,0) = \varphi(x), \end{aligned} \tag{10}$$

where $\alpha(t)$ and $\beta(x,t)$ are bounded real functions, $p \geqslant 3$, was introduced and investigated in [17,43] and references therein. This is a special case of problem (1) since one could choose

$$\Psi\left(|\psi|^2, x, t\right) = \frac{2\beta(x,t)}{p+1}|\psi|^{p+1}.$$

In the case when $\alpha(t)$ and $\beta(x,t)$ are constant functions, there has been lots of research and results from both the theoretical and numerical point of view (see, for instance, [1,7–9,14,15,17,21,24,36,37, 39–42,45]). Some useful and well-known numerical schemes and their conservative properties have been proposed and analyzed in [9,22,41,45]. For instance, the scheme

$$\begin{aligned} &\frac{\mathrm{i}}{\Delta t}(\psi_{j,k+1} - \psi_{j,k}) + \frac{\alpha}{2\Delta x^2}\left((\psi_{j+1,k+1} - 2\psi_{j,k+1} + \psi_{j-1,k+1}) + (\psi_{j+1,k} - 2\psi_{j,k} + \psi_{j-1,k})\right) \\ &\quad + \frac{\beta}{p+1}\frac{|\psi_{j,k+1}|^{p+1} - |\psi_{j,k}|^{p+1}}{|\psi_{j,k+1}|^2 - |\psi_{j,k}|^2}(\psi_{j,k+1} + \psi_{j,k}) = 0, \end{aligned} \tag{11}$$

was considered in [9].

A natural extension of the above scheme (11) to (10), is

$$\frac{\mathrm{i}}{\Delta t}(\psi_{j,k+1}-\psi_{j,k})+\frac{\alpha(t_{k+\frac{1}{2}})}{2\Delta x^2}\big((\psi_{j+1,k+1}-2\psi_{j,k+1}+\psi_{j-1,k+1})+(\psi_{j+1,k}-2\psi_{j,k}+\psi_{j-1,k})\big)$$
$$+\frac{\beta(x_j,t_{k+\frac{1}{2}})}{p+1}\left(\frac{|\psi_{j,k+1}|^{p+1}-|\psi_{j,k}|^{p+1}}{|\psi_{j,k+1}|^2-|\psi_{j,k}|^2}\right)(\psi_{j,k+1}+\psi_{j,k})=0, \tag{12}$$

that can regarded as a special case of the modified Crank–Nicolson scheme (4) (in short, denoted by **MCN**).

A generalization of the Goldberg scheme to the nonlinear equation (10) is

$$\frac{\mathrm{i}}{\Delta t}(\psi_{j,k+1}-\psi_{j,k})+\frac{\alpha(t_{k+\frac{1}{2}})}{2\Delta x^2}\big((\psi_{j+1,k+1}-2\psi_{j,k+1}+\psi_{j-1,k+1})+(\psi_{j+1,k}-2\psi_{j,k}+\psi_{j-1,k})\big)$$
$$+\beta(x_j,t_{k+\frac{1}{2}})|\psi_{j,k+\frac{1}{2}}|^{p-1}\psi_{j,k+\frac{1}{2}}=0,$$

which is denoted by **MG**.

The result below follows as a corollary of Proposition 1 applied to (10).

Proposition 3.

(1) $E_1(\psi)=\int_{\mathbb{R}}|\psi|^2\,dx=E_1(\varphi)$;
(2) *If* $\alpha=$ *constant and* $\beta(x,t)$ *is independent of* t, *then*

$$E_2(\psi)=\int_{\mathbb{R}}\left(\alpha|\psi_x|^2-\frac{2\beta(x)}{p+1}|\psi|^{p+1}\right)dx=E_2(\varphi), \tag{13}$$

where $E_2(\varphi)=\int_{\mathbb{R}}(\alpha|\varphi_x|^2-\frac{2\beta(x)}{p+1}|\varphi|^{p+1})\,dx$.

2. A multi-symplectic scheme

Now we turn our attention to an intrinsic conservative property—multi-symplecticity—of the equation in problem (1) and the difference scheme which preserves the property. The importance of multi-symplectic integrators proposed in [4,5,7,8,18,29–31,37] is the exact preservation of multi-symplectic structure in numerical computation for infinite-dimensional Hamiltonian systems involving Schrödinger equations with constant coefficients. The multi-symplecticity in [4,5] (also, in [7,8,18] and, equivalently, [29–31,37]) is one of the most useful tool for construction of multi-symplectic integrators in the case of constant coefficients. In this section we firstly extend Bridge–Reich definition of multi-symplectic integrator in [4,5,7,8,18] to the case of variable coefficients, then derive a multi-symplectic integrator for the equation in problem (1).

Consider the Schrödinger equation in problem (1) and let $\psi(x,t)=u(x,t)+\mathrm{i}v(x,t)$. Then, the equation in (1) is equivalent to

$$\begin{cases}-\frac{\partial v}{\partial t}+\alpha(t)\frac{\partial^2 u}{\partial x^2}+\Psi'_{|\psi|^2}(|\psi|^2,x,t)u=0,\\ \frac{\partial u}{\partial t}+\alpha(t)\frac{\partial^2 v}{\partial x^2}+\Psi'_{|\psi|^2}(|\psi|^2,x,t)v=0,\end{cases} \tag{14}$$

as it can be easily verified by setting both real and imaginary part equal to zero.

Set $z = (u, v, u_x, v_x)^{\mathrm{T}}$. Eq. (14) can be rewritten as

$$M\frac{\partial z}{\partial t} + K(t)\frac{\partial z}{\partial x} = \nabla_z S(z, x, t), \tag{15}$$

where

$$M = \begin{pmatrix} 0 & -1 & 0 & 0 \\ 1 & 0 & 0 & 0 \\ 0 & 0 & 0 & 0 \\ 0 & 0 & 0 & 0 \end{pmatrix}, \qquad K(t) = \alpha(t) \begin{pmatrix} 0 & 0 & 1 & 0 \\ 0 & 0 & 0 & 1 \\ -1 & 0 & 0 & 0 \\ 0 & -1 & 0 & 0 \end{pmatrix},$$

and

$$S(z, x, t) = -\frac{1}{2}\Psi\left(u^2 + v^2, x, t\right) - \frac{\alpha(t)}{2}\left(u_x^2 + v_x^2\right).$$

It is easy to check that

$$\frac{\partial \omega}{\partial t} + \frac{\partial \kappa}{\partial x} = 0 \tag{16}$$

for the differential forms $\omega(U, V) = \langle MU, V\rangle$ and $\kappa(U, V) = \langle K(t)U, V\rangle$, where $U(x, t)$ and $V(x, t)$ are the solutions of the variational equation of (15)

$$M\frac{\partial (dz)}{\partial t} + K(t)\frac{\partial (dz)}{\partial x} = D_{zz}S(z, x, t)(dz), \tag{17}$$

$\langle \cdot, \cdot \rangle$ is the inner product, and $D_{zz}S$ is the second order derivative of S with respect to z (a symmetric matrix function). Eq. (16) is an intrinsic conservation law for (15) and for (1).

Next, we turn our attention to the numerical discretization of (15), which preserves (16) in the discrete sense. Eqs. (15)–(17) can be discretized as

$$M\partial_t^{j,k} z_{j,k} + K^k \partial_x^{j,k} z_{j,k} = (\nabla_z S_{j,k})_{j,k}, \tag{18}$$

$$\partial_t^{j,k} \omega_{j,k} + \partial_x^{j,k} \kappa_{j,k} = 0, \tag{19}$$

$$M\partial_t^{j,k}(dz)_{j,k} + K^k \partial_x^{j,k}(dz)_{j,k} = \left(D_{zz}^{j,k} S_{j,k}\right)(dz)_{j,k}, \tag{20}$$

where $S_{j,k} = S(z_{j,k}, x_j, t_k)$, $K^k = K(t_k)$, and

$$\omega_{j,k} = \langle MU_{j,k}, V_{j,k}\rangle, \qquad \kappa_{j,k} = \left\langle K^k U_{j,k}, V_{j,k}\right\rangle,$$

with $U_{j,k}$ and $V_{j,k}$ being solutions of (20), and $\partial_t^{j,k}$, $\partial_x^{j,k}$ being discretizations of the derivatives ∂_t and ∂_x, respectively.

Definition 1. The numerical scheme (18) is said to be *multi-symplectic* if (19) is a discrete conservation law of (18).

As we have mentioned before, multi-symplecticity for autonomous and constant coefficient equations has been investigated at large in the last few years (see [4,5,7,8,16–18,21,29–31,37] and references therein)—in particular, the central box scheme is multi-symplectic for autonomous problems. In [7,8,18], some applications of the central box scheme to autonomous systems are presented.

In what follows, we apply the central box scheme to the variable-coefficient case (15). The formulas corresponding to (18)–(20) are

$$M\delta_t z_{j+\frac{1}{2},k} + K^{k+\frac{1}{2}}\delta_x z_{j,k+\frac{1}{2}} = \nabla_z S(z_{j+\frac{1}{2},k+\frac{1}{2}}, x_{j+\frac{1}{2}}, t_{k+\frac{1}{2}}), \tag{21}$$

$$\delta_t \omega_{j+\frac{1}{2},k} + \delta_x \kappa_{j,k+\frac{1}{2}} = 0, \tag{22}$$

$$M\delta_t\, dz_{j+\frac{1}{2},k} + K^{k+\frac{1}{2}}\delta_x\, dz_{j,k+\frac{1}{2}} = A_{j+\frac{1}{2},k+\frac{1}{2}}\, dz_{j+\frac{1}{2},k+\frac{1}{2}}, \tag{23}$$

where

$$A_{j+\frac{1}{2},k+\frac{1}{2}} = D_{zz}S_{j+\frac{1}{2},k+\frac{1}{2}},$$
$$\delta_t z_{j,k} = \frac{1}{\Delta t}(z_{j,k+1} - z_{j,k}),$$
$$\delta_x z_{j,k} = \frac{1}{\Delta x}(z_{j+1,k} - z_{j,k}),$$
$$\omega_{j,k} = \langle MU_{j,k}, V_{j,k}\rangle,$$
$$\kappa_{j,k} = \langle K^k U_{j,k}, V_{j,k}\rangle$$

and $U_{j,k}$ and $V_{j,k}$ are the solutions of (23). From

$$\langle A_{j+\frac{1}{2},k+\frac{1}{2}}U_{j+\frac{1}{2},k+\frac{1}{2}}, V_{j+\frac{1}{2},k+\frac{1}{2}}\rangle - \langle A_{j+\frac{1}{2},k+\frac{1}{2}}V_{j+\frac{1}{2},k+\frac{1}{2}}, U_{j+\frac{1}{2},k+\frac{1}{2}}\rangle = 0 \tag{24}$$

and the skew-symmetry of M and $K(t)$, the result below follows.

Theorem 1. *The central box scheme* (21) *is multi-symplectic*: *Eq.* (22) *is satisfied in each box.*

Note that (21) is a generalization of result in [5] to the varying coefficient case. The use of (21) is not straightforward and convenient in the presence of initial and boundary conditions. An alternative is to produce a numerical scheme which only depends on ψ, and this is done by eliminating the u_x, v_x variables in (21) by standard algebraic procedures.

To this goal, note that (21) can be written as

$$-\frac{1}{\Delta t}(v_{j+\frac{1}{2},k+1} - v_{j+\frac{1}{2},k}) + \frac{\alpha(t_{k+\frac{1}{2}})}{\Delta x}\big((u_x)_{j+1,k+\frac{1}{2}} - (u_x)_{j,k+\frac{1}{2}}\big)$$
$$= -\Psi'_{|\psi|^2}\big(|\psi_{j+\frac{1}{2},k+\frac{1}{2}}|^2, x_{j+\frac{1}{2}}, t_{k+\frac{1}{2}}\big)u_{j+\frac{1}{2},k+\frac{1}{2}}, \tag{25}$$

$$\frac{1}{\Delta t}(u_{j+\frac{1}{2},k+1} - u_{j+\frac{1}{2},k}) + \frac{\alpha(t_{k+\frac{1}{2}})}{\Delta x}\big((v_x)_{j+1,k+\frac{1}{2}} - (v_x)_{j,k+\frac{1}{2}}\big)$$
$$= -\Psi'_{|\psi|^2}\big(|\psi_{j+\frac{1}{2},k+\frac{1}{2}}|^2, x_{j+\frac{1}{2}}, t_{k+\frac{1}{2}}\big)v_{j+\frac{1}{2},k+\frac{1}{2}}, \tag{26}$$

$$\frac{1}{\Delta x}(u_{j+1,k+\frac{1}{2}} - u_{j,k+\frac{1}{2}}) = (u_x)_{j+\frac{1}{2},k+\frac{1}{2}}, \tag{27}$$

$$\frac{1}{\Delta x}(v_{j+1,k+\frac{1}{2}} - v_{j,k+\frac{1}{2}}) = (v_x)_{j+\frac{1}{2},k+\frac{1}{2}}. \tag{28}$$

It seems that the numerical experiment in [21] has been done by using (25)–(28). In order to make numerical implementation a little bit cheaper, now we derive a multi-symplectic scheme corresponding to the original equation in problem (1).

From (27) and (28) it follows that

$$\frac{1}{\Delta x}(u_{j+1,k+\frac{1}{2}} - 2u_{j,k+\frac{1}{2}} + u_{j-1,k+\frac{1}{2}}) = \frac{1}{2}\big((u_x)_{j+1,k+\frac{1}{2}} - (u_x)_{j-1,k+\frac{1}{2}}\big), \tag{29}$$

$$\frac{1}{\Delta x}(v_{j+1,k+\frac{1}{2}} - 2v_{j,k+\frac{1}{2}} + v_{j-1,k+\frac{1}{2}}) = \frac{1}{2}\big((v_x)_{j+1,k+\frac{1}{2}} - (v_x)_{j-1,k+\frac{1}{2}}\big). \tag{30}$$

Thus, we obtain

$$\begin{aligned}
&-\frac{1}{\Delta t}\big((v_{j+\frac{1}{2},k+1} - v_{j+\frac{1}{2},k}) + (v_{j-\frac{1}{2},k+1} - v_{j-\frac{1}{2},k})\big) + \frac{2\alpha(t_{k+\frac{1}{2}})}{\Delta x^2}(u_{j+1,k+\frac{1}{2}} - 2u_{j,k+\frac{1}{2}} + u_{j-1,k+\frac{1}{2}}) \\
&\quad = -\Psi'_{|\psi|^2}\big(|\psi_{j+\frac{1}{2},k+\frac{1}{2}}|^2, x_{j+\frac{1}{2}}, t_{k+\frac{1}{2}}\big)u_{j+\frac{1}{2},k+\frac{1}{2}} - \Psi'_{|\psi|^2}\big(|\psi_{j-\frac{1}{2},k+\frac{1}{2}}|^2, x_{j-\frac{1}{2}}, t_{k+\frac{1}{2}}\big)u_{j-\frac{1}{2},k+\frac{1}{2}},
\end{aligned} \tag{31}$$

$$\begin{aligned}
&\frac{1}{\Delta t}\big((u_{j+\frac{1}{2},k+1} - u_{j+\frac{1}{2},k}) + (u_{j-\frac{1}{2},k+1} - u_{j-\frac{1}{2},k})\big) + \frac{2\alpha(t_{k+\frac{1}{2}})}{\Delta x^2}(v_{j+1,k+\frac{1}{2}} - 2v_{j,k+\frac{1}{2}} + v_{j-1,k+\frac{1}{2}}) \\
&\quad = -\Psi'_{|\psi|^2}\big(|\psi_{j+\frac{1}{2},k+\frac{1}{2}}|^2, x_{j+\frac{1}{2}}, t_{k+\frac{1}{2}}\big)v_{j+\frac{1}{2},k+\frac{1}{2}} - \Psi'_{|\psi|^2}\big(|\psi_{j-\frac{1}{2},k+\frac{1}{2}}|^2, x_{j-\frac{1}{2}}, t_{k+\frac{1}{2}}\big)v_{j-\frac{1}{2},k+\frac{1}{2}}.
\end{aligned} \tag{32}$$

Combining the above two equations, we derive the following multi-symplectic scheme

$$\begin{aligned}
&\mathrm{i}(\delta_t\psi_{j-1,k} + 2\delta_t\psi_{j,k} + \delta_t\psi_{j+1,k}) + 2\alpha(t_{k+\frac{1}{2}})\big(\delta_x^2\psi_{j,k} + \delta_x^2\psi_{j,k+1}\big) \\
&\quad + 2\Psi'_{|\psi|^2}\big(|\psi_{j+\frac{1}{2},k+\frac{1}{2}}|^2, x_{j+\frac{1}{2}}, t_{k+\frac{1}{2}}\big)\psi_{j+\frac{1}{2},k+\frac{1}{2}} + 2\Psi'_{|\psi|^2}\big(|\psi_{j-\frac{1}{2},k+\frac{1}{2}}|^2, x_{j-\frac{1}{2}}, t_{k+\frac{1}{2}}\big)\psi_{j-\frac{1}{2},k+\frac{1}{2}} = 0,
\end{aligned} \tag{33}$$

with difference operators

$$\delta_t\psi_{j,k} = \frac{1}{\Delta t}(\psi_{j,k+1} - \psi_{j,k}), \tag{34}$$

$$\delta_x^2\psi_{j,k} = \frac{1}{\Delta x^2}(\psi_{j+1,k} - 2\psi_{j,k} + \psi_{j-1,k}). \tag{35}$$

Obviously, the numerical computation implemented by (33) should be cheaper than by (25)–(28). In [5] it is shown that the scheme (33) preserves energy locally for constant coefficients if S in (15) is quadratic in z.

If $\Psi(|\psi|^2, x, t) = V(x,t)|\psi|^2$, then the scheme (33) becomes

$$\begin{aligned}
&\mathrm{i}(\delta_t\psi_{j-1,k} + 2\delta_t\psi_{j,k} + \delta_t\psi_{j+1,k}) + 2\alpha(t_{k+\frac{1}{2}})\big(\delta_x^2\psi_{j,k} + \delta_x^2\psi_{j,k+1}\big) \\
&\quad + 2V(x_{j+\frac{1}{2}}, t_{k+\frac{1}{2}})\psi_{j+\frac{1}{2},k+\frac{1}{2}} + 2V(x_{j-\frac{1}{2}}, t_{k+\frac{1}{2}})\psi_{j-\frac{1}{2},k+\frac{1}{2}} = 0.
\end{aligned} \tag{36}$$

If $\Psi(|\psi|^2, x, t) = \frac{2\beta(x,t)}{p+1}|\psi|^{p+1}$, $p \geqslant 3$, then the scheme (33) reads

$$\begin{aligned}
&\mathrm{i}(\delta_t\psi_{j-1,k} + 2\delta_t\psi_{j,k} + \delta_t\psi_{j+1,k}) + 2\alpha(t_{k+\frac{1}{2}})\big(\delta_x^2\psi_{j,k} + \delta_x^2\psi_{j,k+1}\big) \\
&\quad + 2\beta(x_{j+\frac{1}{2}}, t_{k+\frac{1}{2}})|\psi_{j+\frac{1}{2},k+\frac{1}{2}}|^{p-1}\psi_{j+\frac{1}{2},k+\frac{1}{2}} + 2\beta(x_{j-\frac{1}{2}}, t_{k+\frac{1}{2}})|\psi_{j-\frac{1}{2},k+\frac{1}{2}}|^{p-1}\psi_{j-\frac{1}{2},k+\frac{1}{2}} = 0.
\end{aligned} \tag{37}$$

An equivalent multi-symplectic conservation law to (16) is

$$\partial_t(du \wedge dv) + \alpha(t)(du_x \wedge du + dv_x \wedge dv) = 0,$$

which can be used (see [21,37]) to show that a higher order multi-symplectic integrator can be produced by application of a pair of Gauss–Legendre collocation methods in time and in space, respectively. In particular, we can apply it to verify that the scheme (4) is not multi-symplectic for some Ψ. Also, it can be shown easily that Goldberg's scheme (9) (and MG scheme) is multi-symplectic.

We will show that (33), (36) and (37) are unitary, which also implies stability with respect to the initial value (see [20,45]). The schemes also possess other global conservation properties that will be investigated in the next section.

3. Conservative properties of the multi-symplectic scheme

The scope of this section is to show that the numerical schemes introduced above possess discrete conservation laws analogous to the continuous ones. Some results (Theorems 2 and 3) in this section, in fact, can be regarded as consequences of discrete Noether theorem [5,29]. *As well known, in the case of Hamiltonian ODEs symplectic integrators may not preserve quadratic invariants* (*see* [38]). In this section we also give a global energy transit formula of the multi-symplectic scheme. In what follows we assume that all sums under considerations are finite.

Theorem 2. *The scheme* (33) (*thus* (36) *and* (37)) *possesses the discrete global conservation law*

$$\|\psi_k\|_{\frac{1}{2}}^2 = \Delta x \sum_j |\psi_{j-\frac{1}{2},k}|^2 = \Delta x \sum_j |\varphi_{j-\frac{1}{2}}|^2 = \|\varphi\|_{\frac{1}{2}}^2, \tag{38}$$

that is, the scheme is unitary, thus stable with respect to the initial value.

Proof. We multiply (33) by $\bar{\psi}_{j,k+1} + \bar{\psi}_{j,k}$, where $\bar{\psi}$ is the complex conjugate of ψ. Then, the first term becomes

$$\begin{aligned}
&\frac{\mathrm{i}}{\Delta t}\big(\psi_{j-1,k+1}\bar{\psi}_{j,k+1} - \psi_{j-1,k}\bar{\psi}_{j,k+1} + \psi_{j-1,k+1}\bar{\psi}_{j,k} - \psi_{j-1,k}\bar{\psi}_{j,k} \\
&\quad + 2|\psi_{j,k+1}|^2 - 2|\psi_{j,k}|^2 + 4\mathrm{i}\Im(\psi_{j,k+1}\bar{\psi}_{j,k}) \\
&\quad + \psi_{j+1,k+1}\bar{\psi}_{j,k+1} + \psi_{j+1,k+1}\bar{\psi}_{j,k} - \psi_{j+1,k}\bar{\psi}_{j,k+1} - \psi_{j+1,k}\bar{\psi}_{j,k}\big)
\end{aligned} \tag{39}$$

(as usual, $\Re$, $\Im$ stand for 'real' and 'imaginary' part, respectively). The second term in (33) reads

$$\begin{aligned}
&\frac{2\alpha(t_{k+\frac{1}{2}})}{(\delta x)^2}\big(\psi_{j+1,k+1}\bar{\psi}_{j,k+1} - 2|\psi_{j,k+1}|^2 + \psi_{j-1,k+1}\bar{\psi}_{j,k+1} \\
&\quad + \psi_{j+1,k+1}\bar{\psi}_{j,k} - 2\psi_{j,k+1}\bar{\psi}_{j,k} + \psi_{j-1,k+1}\bar{\psi}_{j,k} + \psi_{j+1,k}\bar{\psi}_{j,k+1} - 2\psi_{j,k}\bar{\psi}_{j,k+1} + \psi_{j-1,k}\bar{\psi}_{j,k+1} \\
&\quad + \psi_{j+1,k}\bar{\psi}_{j,k} - 2|\psi_{j,k}|^2 + \psi_{j-1,k}\bar{\psi}_{j,k}\big).
\end{aligned} \tag{40}$$

The third and fourth in (33) yield

$$\begin{aligned}
&2(\Theta_{j-\frac{1}{2},k+\frac{1}{2}}\psi_{j-\frac{1}{2},k+\frac{1}{2}} + \Theta_{j+\frac{1}{2},k+\frac{1}{2}}\psi_{j+\frac{1}{2},k+\frac{1}{2}})\bar{\psi}_{j,k+\frac{1}{2}} \\
&\quad = \Theta_{j-\frac{1}{2},k+\frac{1}{2}}|\psi_{j,k+\frac{1}{2}}|^2 + \Theta_{j-\frac{1}{2},k+\frac{1}{2}}\psi_{j-1,k+\frac{1}{2}}\bar{\psi}_{j,k+\frac{1}{2}} \\
&\qquad + \Theta_{j+\frac{1}{2},k+\frac{1}{2}}|\psi_{j,k+\frac{1}{2}}|^2 + \Theta_{j+\frac{1}{2},k+\frac{1}{2}}\psi_{j+1,k+\frac{1}{2}}\bar{\psi}_{j,k+\frac{1}{2}} \\
&\quad = (\Theta_{j-\frac{1}{2},k+\frac{1}{2}} + \Theta_{j+\frac{1}{2},k+\frac{1}{2}})|\psi_{j,k+\frac{1}{2}}|^2 \\
&\qquad + \psi_{j-1,k+\frac{1}{2}}(\Theta_{j-\frac{1}{2},k+\frac{1}{2}}\bar{\psi}_{j,k+\frac{1}{2}}) + (\Theta_{j+\frac{1}{2},k+\frac{1}{2}}\psi_{j+1,k+\frac{1}{2}})\bar{\psi}_{j,k+\frac{1}{2}},
\end{aligned} \tag{41}$$

where $\Theta_{j,k} = \Theta(\psi_{j,k}, x_j, t_k) = \Psi'_{|\psi|^2}(|\psi_{j,k}|^2, x_j, t_k)$.

Next, we sum over j and take the imaginary part. It follows that (40) and (41) yield real functions, respectively. Furthermore, Eq. (39) yields

$$\Delta x \sum_j |\psi_{j,k+1}|^2 + \Delta x \Re \sum_j (\psi_{j-1,k+1}\bar{\psi}_{j,k+1}) = \Delta x \sum_j |\varphi_j|^2 + \Delta x \Re \sum_j (\varphi_{j-1}\bar{\varphi}_j),$$
$$\Delta x \sum_j |\psi_{j-1,k+1}|^2 + \Delta x \Re \sum_j (\psi_{j-1,k+1}\bar{\psi}_{j,k+1}) = \Delta x \sum_j |\varphi_{j-1}|^2 + \Delta x \Re \sum_j (\varphi_{j-1}\bar{\varphi}_j). \tag{42}$$

This implies

$$\|\psi_k\|_{\frac{1}{2}}^2 = \Delta x \sum_j |\psi_{j-\frac{1}{2},k}|^2 = \Delta x \sum_j |\varphi_{j-\frac{1}{2}}|^2 = \|\varphi\|_{\frac{1}{2}}^2, \tag{43}$$

which is consistent with the first conservation law in Proposition 1, a global discrete conservation law and a discrete ergodicity in spatial direction. This completes the proof. □

Remark 1.

1. In the quantum case (see Section 1.2), the theorem tell us that the quantum normalization is preserved by the multi-symplectic scheme (36).
2. The scheme (33) does not satisfy $\|\psi_k\|^2 = \|\varphi\|^2$ (the global norm conservation at mesh points). This means that the discrete global norm conservation of (33) is only in the sense of that corresponding discretization.
3. By using similar method, one can show that the discrete global momentum is preserved by the multi-symplectic integrator in the sense of the corresponding discretization.

The next result concerns Hamiltonian conservation and the global energy transit formula in the temporal direction (especially relevant in the quantum physics context).

Theorem 3. *If $\alpha(t) \equiv$ constant and V is independent of t, then the scheme* (36) *satisfies the discrete global energy conservation law*

$$\Delta x \sum_j \left(\alpha \left| \frac{\psi_{j,k} - \psi_{j-1,k}}{\Delta x} \right|^2 - V_{j-\frac{1}{2}} |\psi_{j-\frac{1}{2},k}|^2 \right) = \Delta x \sum_j \left(\alpha \left| \frac{\varphi_j - \varphi_{j-1}}{\Delta x} \right|^2 - V_{j-\frac{1}{2}} |\varphi_{j-\frac{1}{2}}|^2 \right). \tag{44}$$

Moreover, in this case, the discrete global energy of (36) *is*

$$\Delta x \sum_j \left(\alpha \left| \frac{\varphi_j - \varphi_{j-1}}{\Delta x} \right|^2 - V_{j-\frac{1}{2}} |\varphi_{j-\frac{1}{2}}|^2 \right).$$

Proof. We multiply (36) by $(\bar{\psi}_{j,k+1} - \bar{\psi}_{j,k})$. The first term becomes

$$\frac{i}{\Delta t} \big(\psi_{j+1,k+1}\bar{\psi}_{j,k+1} - \psi_{j+1,k}\bar{\psi}_{j,k+1} - \psi_{j+1,k+1}\bar{\psi}_{j,k} + \psi_{j+1,k}\bar{\psi}_{j,k} + 2|\psi_{j,k+1} - \psi_{j,k}|^2 + \psi_{j-1,k+1}\bar{\psi}_{j,k+1} - \psi_{j-1,k}\bar{\psi}_{j,k+1} - \psi_{j-1,k+1}\bar{\psi}_{j,k} + \psi_{j-1,k}\bar{\psi}_{j,k} \big). \tag{45}$$

The second term in (36) becomes

$$\frac{2\alpha}{(\Delta x)^2}\big(\psi_{j+1,k+1}\bar{\psi}_{j,k+1} - 2|\psi_{j,k+1}|^2 + \psi_{j-1,k+1}\bar{\psi}_{j,k+1} - \psi_{j+1,k+1}\bar{\psi}_{j,k} + 2\psi_{j,k+1}\bar{\psi}_{j,k}$$
$$- \psi_{j-1,k+1}\bar{\psi}_{j,k} + \psi_{j+1,k}\bar{\psi}_{j,k+1} - 2\psi_{j,k}\bar{\psi}_{j,k+1} + \psi_{j-1,k}\bar{\psi}_{j,k+1}$$
$$- \psi_{j+1,k}\bar{\psi}_{j,k} + 2|\psi_{j,k}|^2 - \psi_{j-1,k}\bar{\psi}_{j,k}\big). \tag{46}$$

The third and fourth terms in (36) yield

$$\frac{1}{2}V_{j-\frac{1}{2}}\big(|\psi_{j,k+1}|^2 + \psi_{j-1,k+1}\bar{\psi}_{j,k+1} + \psi_{j,k}\bar{\psi}_{j,k+1} + \psi_{j-1,k}\bar{\psi}_{j,k+1}$$
$$- \psi_{j,k+1}\bar{\psi}_{j,k} - \psi_{j-1,k+1}\bar{\psi}_{j,k} - |\psi_{j,k}|^2 - \psi_{j-1,k}\bar{\psi}_{j,k}\big)$$
$$+ \frac{1}{2}V_{j+\frac{1}{2}}\big(|\psi_{j,k+1}|^2 + \psi_{j+1,k+1}\bar{\psi}_{j,k+1} + \psi_{j+1,k}\bar{\psi}_{j,k+1} + \psi_{j,k}\bar{\psi}_{j,k+1}$$
$$- \psi_{j+1,k+1}\bar{\psi}_{j,k} - \psi_{j,k+1}\bar{\psi}_{j,k} - |\psi_{j,k}|^2 - \psi_{j+1,k}\bar{\psi}_{j,k}\big). \tag{47}$$

Now we sum (45), (46) and (47) over j, then take real parts. Eq. (45) vanishes. It follows from (46) that

$$\frac{2\alpha}{\Delta x^2}\bigg(\sum_j\big(-2|\psi_{j-1,k+1}|^2 + 2|\psi_{j,k}|^2\big) + \sum_j \psi_{j+1,k+1}\bar{\psi}_{j,k+1} + \sum_j \psi_{j-1,k+1}\bar{\psi}_{j,k+1}$$
$$- \sum_j \psi_{j+1,k}\bar{\psi}_{j,k} - \sum_j \psi_{j-1,k}\bar{\psi}_{j,k} + 2\sum_j(\psi_{j,k+1}\bar{\psi}_{j,k} - \psi_{j,k}\bar{\psi}_{j,k+1})$$
$$- \sum_j \psi_{j-1,k+1}\bar{\psi}_{j,k} + \sum_j \psi_{j+1,k}\bar{\psi}_{j,k+1} - \sum_j \psi_{j+1,k+1}\bar{\psi}_{j,k} + \sum_j \psi_{j-1,k}\bar{\psi}_{j,k+1}\bigg)$$
$$= \frac{2\alpha}{\Delta x^2}\bigg(\sum_j\big(-2|\psi_{j-1,k+1}|^2 + 2|\psi_{j,k}|^2\big) + 2\sum_j \Re(\psi_{j-1,k+1}\bar{\psi}_{j,k+1})$$
$$- 2\sum_j \Re(\psi_{j-1,k}\bar{\psi}_{j,k}) + 4\mathrm{i}\sum_j \Im(\psi_{j-1,k}\bar{\psi}_{j-1,k+1}) + 2\mathrm{i}\sum_j \Im(\psi_{j,k}\bar{\psi}_{j-1,k+1} + \psi_{j-1,k}\bar{\psi}_{j,k+1})\bigg),$$

thus its real part is

$$\frac{2\alpha}{(\Delta x)^2}\sum_j\big(-2|\psi_{j,k+1}|^2 + 2\Re(\psi_{j,k+1}\bar{\psi}_{j+1,k+1}) + 2|\psi_{j,k}|^2 - 2\Re(\psi_{j,k}\bar{\psi}_{j+1,k})\big)$$
$$= 2\alpha\sum_j\left(\left|\frac{\psi_{j,k} - \psi_{j-1,k}}{\Delta x}\right|^2 - \left|\frac{\psi_{j,k+1} - \psi_{j-1,k+1}}{\Delta x}\right|^2\right). \tag{48}$$

From (47), we get

$$\frac{1}{2}\bigg(\sum_j V_{j-\frac{1}{2}}\big(|\psi_{j,k+1}|^2 + \psi_{j-1,k+1}\bar{\psi}_{j,k+1} - |\psi_{j,k}|^2 - \psi_{j-1,k}\bar{\psi}_{j,k}\big)$$
$$+ \sum_j V_{j-\frac{1}{2}}2\mathrm{i}\Im(\psi_{j,k}\bar{\psi}_{j,k+1}) + \sum_j V_{j-\frac{1}{2}}\psi_{j-1,k}\bar{\psi}_{j,k+1} - \sum_j V_{j-\frac{1}{2}}\psi_{j-1,k+1}\bar{\psi}_{j,k}$$

$$+\sum_j V_{j+\frac{1}{2}}\big(|\psi_{j,k+1}|^2+\psi_{j+1,k+1}\bar{\psi}_{j,k+1}-|\psi_{j,k}|^2-\psi_{j+1,k}\bar{\psi}_{j,k}\big)$$

$$+\sum_j V_{j+\frac{1}{2}}2\mathrm{i}\Im(\psi_{j,k}\bar{\psi}_{j,k+1})+\sum_j V_{j+\frac{1}{2}}\psi_{j+1,k}\bar{\psi}_{j,k+1}-\sum_j V_{j+\frac{1}{2}}\psi_{j+1,k+1}\bar{\psi}_{j,k}\Big),$$

hence its real part is

$$\begin{aligned}
&\frac{1}{2}\Big(\sum_j V_{j-\frac{1}{2}}\big(|\psi_{j,k+1}|^2+\Re(\psi_{j-1,k+1}\bar{\psi}_{j,k+1})-|\psi_{j,k}|^2-\Re(\psi_{j-1,k}\bar{\psi}_{j,k})\big)\\
&\quad+\sum_j V_{j+\frac{1}{2}}\big(|\psi_{j,k+1}|^2+\Re(\psi_{j+1,k+1}\bar{\psi}_{j,k+1})-|\psi_{j,k}|^2-\Re(\psi_{j+1,k}\bar{\psi}_{j,k})\big)\Big)\\
&=\frac{1}{2}\sum_j V_{j-\frac{1}{2}}\big(\big(|\psi_{j,k+1}|^2+|\psi_{j-1,k+1}|^2+2\Re(\psi_{j-1,k+1}\bar{\psi}_{j,k+1})\big)\\
&\quad-\big(|\psi_{j,k}|^2+|\psi_{j-1,k}|^2+2\Re(\psi_{j-1,k}\bar{\psi}_{j,k})\big)\big)\\
&=2\sum_j V_{j-\frac{1}{2}}\big(|\psi_{j-\frac{1}{2},k+1}|^2-|\psi_{j-\frac{1}{2},k}|^2\big). \qquad (49)
\end{aligned}$$

Combining (48) and (49), we obtain

$$\alpha\sum_j\left(\left|\frac{\psi_{j,k}-\psi_{j-1,k}}{\Delta x}\right|^2-\left|\frac{\psi_{j,k+1}-\psi_{j-1,k+1}}{\Delta x}\right|^2\right)+\sum_j V_{j-\frac{1}{2}}\big(|\psi_{j-\frac{1}{2},k+1}|^2-|\psi_{j-\frac{1}{2},k}|^2\big)=0, \quad (50)$$

hence (44), which completes the proof. □

The three results below have similar proofs (which we therefore omit).

Theorem 4. *The scheme* (33) *satisfies the implicit discrete global conservation law*

$$\begin{aligned}
&\alpha(t_{k+\frac{1}{2}})\sum_j\left(\left|\frac{\psi_{j,k}-\psi_{j-1,k}}{\Delta x}\right|^2-\left|\frac{\psi_{j,k+1}-\psi_{j-1,k+1}}{\Delta x}\right|^2\right)\\
&\quad+\sum_j \Theta_{j-\frac{1}{2},k+\frac{1}{2}}\big(|\psi_{j-\frac{1}{2},k+1}|^2-|\psi_{j-\frac{1}{2},k}|^2\big)=0, \qquad (51)
\end{aligned}$$

where $\Theta(\psi,x,t)=\Psi'_{|\psi|^2}(|\psi|^2,x,t)$, *and* $\Theta_{j,k}=\Theta(\psi_{j,k},x_j,t_k)$.

Theorem 5. *If* $\alpha\equiv$ *constant and* Θ *is independent of* ψ *and* t, *the scheme* (33) *admits*

$$\alpha\sum_j\left|\frac{\psi_{j,k}-\psi_{j-1,k}}{\Delta x}\right|^2-\sum_j\Theta_{j-\frac{1}{2}}|\psi_{j-\frac{1}{2},k}|^2=\alpha\sum_j\left|\frac{\varphi_j-\varphi_{j-1}}{\Delta x}\right|^2-\sum_j\Theta_{j-\frac{1}{2}}|\varphi_{j-\frac{1}{2}}|^2, \quad (52)$$

where $\Theta(\psi,x)=\Psi'_{|\psi|^2}(|\psi|^2,x)$, *and* $\Theta_{j,k}=\Theta(\psi_{j,k},x_j)$.

Theorem 6. *The numerical scheme* (4) *and the MG scheme have the following discrete global conservation laws*

$$\|\psi_k\|^2 = \Delta x \sum_j |\psi_{j,k}|^2 = \Delta x \sum_j |\varphi_j|^2 = \|\varphi\|^2. \tag{53}$$

Theorem 4 tells us that the variation of global energy of (33) is not explicitly conservative in time evolution, and the transit of global energy in temporal direction obeys (51). For example, let $\alpha \equiv 1$, and $\Psi'_{|\psi|^2}(|\psi|^2, x, t) = |\psi|^2$. Then the discrete global energy should be

$$E(t_k) = \Delta x \sum_j \left(\left| \frac{\psi_{j+1,k} - \psi_{j,k}}{\Delta x} \right|^2 - \frac{1}{2} \left| \frac{\psi_{j+1,k} + \psi_{j,k}}{2} \right|^4 \right). \tag{54}$$

Thus we have a discrete global energy formula.

Corollary 1. *If* $\alpha \equiv 1$, *and* $\Psi'_{|\psi|^2}(|\psi|^2, x, t) = |\psi|^2$, *then*

$$e_k = E(t_{k+1}) - E(t_k) = \frac{\Delta x}{4} \sum_j |\psi_{j-\frac{1}{2},k+1} - \psi_{j-\frac{1}{2},k}|^2 \big(|\psi_{j-\frac{1}{2},k}|^2 - |\psi_{j-\frac{1}{2},k+1}|^2 \big).$$

Furthermore,

$$E(t_n) = E(t_0) + \frac{\Delta x}{4} \sum_{k=0}^{n} \sum_j |\psi_{j-\frac{1}{2},k+1} - \psi_{j-\frac{1}{2},k}|^2 \big(|\psi_{j-\frac{1}{2},k}|^2 - |\psi_{j-\frac{1}{2},k+1}|^2 \big).$$

Proof. It follows from (51) in Theorem 4 that

$$\begin{aligned}
&E(t_{k+1}) - E(t_k) \\
&\quad = \Delta x \sum_j \left(\left| \frac{\psi_{j+1,k+1} - \psi_{j,k+1}}{\Delta x} \right|^2 - \frac{1}{2} \left| \frac{\psi_{j+1,k+1} + \psi_{j,k+1}}{2} \right|^4 - \left| \frac{\psi_{j+1,k} - \psi_{j,k}}{\Delta x} \right|^2 \right. \\
&\qquad \left. + \frac{1}{2} \left| \frac{\psi_{j+1,k} + \psi_{j,k}}{2} \right|^4 \right) \\
&\quad = \Delta x \sum_j \big(|\psi_{j-\frac{1}{2},k+\frac{1}{2}}|^2 \big(|\psi_{j-\frac{1}{2},k+1}|^2 - |\psi_{j-\frac{1}{2},k}|^2 \big) - \frac{1}{2} |\psi_{j-\frac{1}{2},k+1}|^4 + \frac{1}{2} |\psi_{j-\frac{1}{2},k}|^4 \big) \\
&\quad = \frac{\Delta x}{2} \sum_j \big(|\psi_{j-\frac{1}{2},k+1}|^2 - |\psi_{j-\frac{1}{2},k}|^2 \big) \big(\big(|\psi_{j-\frac{1}{2},k+\frac{1}{2}}|^2 - |\psi_{j-\frac{1}{2},k+1}|^2 \big) + \big(|\psi_{j-\frac{1}{2},k+\frac{1}{2}}|^2 - |\psi_{j-\frac{1}{2},k}|^2 \big) \big) \\
&\quad = \frac{\Delta x}{4} \sum_j |\psi_{j-\frac{1}{2},k+1} - \psi_{j-\frac{1}{2},k}|^2 \big(|\psi_{j-\frac{1}{2},k}|^2 - |\psi_{j-\frac{1}{2},k+1}|^2 \big).
\end{aligned}$$

This completes the proof of the corollary. □

4. Error estimation for the multi-symplectic scheme

In this section we make use of the numerical conservation laws obeyed by the proposed multi-symplectic scheme to estimate the error. We denote by $\hat{\psi}$ the exact solution of (1). Let us assume that

$$\|\hat{\psi}_k\|_{\frac{1}{2}}^2 \leqslant 2E_1(\varphi), \tag{55}$$

and set

$$r_{j,k} = \hat{\psi}_{j,k} - \psi_{j,k}.$$

The latter is the (pointwise) error of the numerical scheme. It follows from Theorem 2 that

$$\|r_k\|_{\frac{1}{2}}^2 \leqslant 8E_1(\varphi). \tag{56}$$

The truncation error of (33) is denoted by

$$\begin{aligned} F_{j-\frac{1}{2},k+\frac{1}{2}} = {} & \frac{\mathrm{i}}{\Delta t}\big((\hat{\psi}_{j+\frac{1}{2},k+1} - \hat{\psi}_{j+\frac{1}{2},k}) + (\hat{\psi}_{j-\frac{1}{2},k+1} - \hat{\psi}_{j-\frac{1}{2},k})\big) \\ & + \frac{2\alpha(t_{k+\frac{1}{2}})}{\Delta x^2}(\hat{\psi}_{j+1,k+\frac{1}{2}} - 2\hat{\psi}_{j,k+\frac{1}{2}} + \hat{\psi}_{j-1,k+\frac{1}{2}}) \\ & + \hat{\Theta}_{j-\frac{1}{2},k+\frac{1}{2}}\hat{\psi}_{j-\frac{1}{2},k+\frac{1}{2}} + \hat{\Theta}_{j+\frac{1}{2},k+\frac{1}{2}}\hat{\psi}_{j+\frac{1}{2},k+\frac{1}{2}}, \end{aligned} \tag{57}$$

where

$$\hat{\Theta}_{j,k} = \Psi'_{|\hat{\psi}|^2}\big(|\hat{\psi}_{j,k}|^2, x_j, t_k\big).$$

Theorem 7. *There exists a positive constant C_1 depending on the initial condition φ only, such that for Δt: $0 < \Delta t < \frac{8}{1+16C_1}$, the errors $\{r_{j,k}\}$ of the multi-symplectic scheme* (33) *satisfy*

$$\begin{aligned} \|r_{k+1}\|_{\frac{1}{2}}^2 \leqslant {} & \frac{1}{8 - \Delta t(1+16C_1)}\left(\big(8 + \Delta t(1+16C_1)\big)\|r_0\|_{\frac{1}{2}}^2 + 2\Delta t\sum_{m=0}^{k}\|F_{m+\frac{1}{2}}\|^2\right) \\ & \times \exp\left(\frac{2k\Delta t(1+16C_1)}{8 - \Delta t(1+16C_1)}\right). \end{aligned} \tag{58}$$

Proof. We substract (33) from (57) to obtain

$$\begin{aligned} & \frac{\mathrm{i}}{\Delta t}\big((r_{j+\frac{1}{2},k+1} - r_{j+\frac{1}{2},k}) + (r_{j-\frac{1}{2},k+1} - r_{j-\frac{1}{2},k})\big) + \frac{2\alpha(t_{k+\frac{1}{2}})}{\Delta x^2}(r_{j+1,k+\frac{1}{2}} - 2r_{j,k+\frac{1}{2}} + r_{j-1,k+\frac{1}{2}}) \\ & \quad = F_{j-\frac{1}{2},k+\frac{1}{2}} + (\Theta_{j-\frac{1}{2},k+\frac{1}{2}} - \hat{\Theta}_{j-\frac{1}{2},k+\frac{1}{2}})\hat{\psi}_{j-\frac{1}{2},k+\frac{1}{2}} - \Theta_{j-\frac{1}{2},k+\frac{1}{2}}r_{j-\frac{1}{2},k+\frac{1}{2}} \\ & \qquad + (\Theta_{j+\frac{1}{2},k+\frac{1}{2}} - \hat{\Theta}_{j+\frac{1}{2},k+\frac{1}{2}})\hat{\psi}_{j+\frac{1}{2},k+\frac{1}{2}} - \Theta_{j+\frac{1}{2},k+\frac{1}{2}}r_{j+\frac{1}{2},k+\frac{1}{2}}, \end{aligned} \tag{59}$$

where $\Theta_{j,k} = \Psi'_{|\psi|^2}(|\psi_{j,k}|^2, x_j, t_k)$.

Multiplying the above equation by $\bar{r}_{j,k+\frac{1}{2}}$, summing over j and taking the imaginary part, one has

$$\frac{2}{\Delta t}\sum_j\left(|r_{j-\frac{1}{2},k+1}|^2-|r_{j-\frac{1}{2},k}|^2\right)$$
$$=\Im\sum_j(F_{j,k+\frac{1}{2}}\bar{r}_{j+\frac{1}{2},k+\frac{1}{2}})+2\sum_j(\Theta_{j-\frac{1}{2},k+\frac{1}{2}}-\hat{\Theta}_{j-\frac{1}{2},k+\frac{1}{2}})\Im(\hat{\psi}_{j-\frac{1}{2},k+\frac{1}{2}}\bar{r}_{j-\frac{1}{2},k+\frac{1}{2}}),\tag{60}$$

where we use

$$\sum_j(F_{j-\frac{1}{2},k+\frac{1}{2}}\bar{r}_{j,k+\frac{1}{2}})=\sum_j(F_{j,k+\frac{1}{2}}\bar{r}_{j+\frac{1}{2},k+\frac{1}{2}}).$$

From our assumptions on Ψ, the boundedness of the exact solution $\hat{\psi}(x,t)$ and Theorem 2, it follows that there exists a constant

$$C_1=\left(\max\left|\hat{\psi}(x,t)\right|\right)\left(\max|\Psi''_{|\psi|^2}|\right)\left(\|\varphi\|^2_{\frac{1}{2}}+\max\left|\hat{\psi}(x,t)\right|\right)>0$$

such that

$$|\Theta_{j-\frac{1}{2},k+\frac{1}{2}}-\hat{\Theta}_{j-\frac{1}{2},k+\frac{1}{2}}|\,|\hat{\psi}_{j-\frac{1}{2},k+\frac{1}{2}}|\leqslant C_1|\bar{r}_{j-\frac{1}{2},k+\frac{1}{2}}|.$$

We have

$$\begin{aligned}\frac{2}{\Delta t}\left|\|r_{k+1}\|^2_{\frac{1}{2}}-\|r_k\|^2_{\frac{1}{2}}\right|&\leqslant\frac{1}{2}\|F_{k+\frac{1}{2}}\|^2_{\frac{1}{2}}+\frac{1}{2}\|r_{k+\frac{1}{2}}\|^2_{\frac{1}{2}}\\&\quad+2\Delta x\sum_j\left|\Theta_{j-\frac{1}{2},k+\frac{1}{2}}-\hat{\Theta}_{j-\frac{1}{2},k+\frac{1}{2}}\|\hat{\psi}_{j-\frac{1}{2},k+\frac{1}{2}}\|\bar{r}_{j-\frac{1}{2},k+\frac{1}{2}}\right|\\&\leqslant\frac{1}{2}\|F_{k+\frac{1}{2}}\|^2_{\frac{1}{2}}+\frac{1+16C_1}{4}\left(\|r_{k+1}\|^2_{\frac{1}{2}}+\|r_k\|^2_{\frac{1}{2}}\right).\end{aligned}\tag{61}$$

This implies that

$$\|r_{k+1}\|^2_{\frac{1}{2}}\leqslant\|r_k\|^2_{\frac{1}{2}}+\frac{\Delta t}{4}\|F_{k+\frac{1}{2}}\|^2+\frac{\Delta t(1+16C_1)}{8}\left(\|r_{k+1}\|^2_{\frac{1}{2}}+\|r_k\|^2_{\frac{1}{2}}\right).\tag{62}$$

Therefore,

$$\begin{aligned}\|r_{k+1}\|^2_{\frac{1}{2}}&\leqslant\|r_0\|^2_{\frac{1}{2}}+\frac{\Delta t}{4}\sum_{m=0}^{k}\|F_{m+\frac{1}{2}}\|^2\\&\quad+\frac{\Delta t(1+16C_1)}{8}\left(\|r_{k+1}\|^2_{\frac{1}{2}}+\|r_0\|^2_{\frac{1}{2}}\right)+\frac{\Delta t(1+16C_1)}{4}\sum_{m=1}^{k}\|r_k\|^2_{\frac{1}{2}}.\end{aligned}\tag{63}$$

By Gronwall's lemma, if $0<\Delta t<\frac{8}{1+16C_1}$, we get

$$\begin{aligned}\|r_{k+1}\|^2_{\frac{1}{2}}&\leqslant\frac{1}{8-\Delta t(1+16C_1)}\left(\left(8+\Delta t(1+16C_1)\right)\|r_0\|^2_{\frac{1}{2}}+2\Delta t\sum_{m=0}^{k}\|F_{m+\frac{1}{2}}\|^2\right)\\&\quad\times\exp\left(\frac{2k\Delta t(1+16C_1)}{8-\Delta t(1+16C_1)}\right).\end{aligned}\tag{64}$$

This completes the proof. □

Remark 2. The inequality (58) implies the numerical error of the scheme (33) is bounded by the initial error and by the truncation error, so the scheme (33) is convergent.

Remark 3. Under our assumption on Ψ and using the corresponding conservative properties in Theorem 5, we also can derive a similar estimation to (58) for the scheme (4), thus the scheme is also convergent.

5. Numerical experiments

On numerical experiments of Schrödinger equations, there have been many references (e.g., [1,2,7–9,11–15,19,21,22,24,25,32,34–36,39–42,45] and references therein) with more details. The main purpose of this section is to compare numerically the multi-symplectic scheme (33) with MG, MCN, by making use of them in numerical simulations of periodic and quasi-periodic solitary-waves. Numerical experiments in [21], with more details on energy, momentum and norm, show that the multi-symplectic integrator preserves the norm and momentum within roundoff. Because the numerical simulation of global momentum conservation is quite similar to that of global norm conservation, based on the work of [21], we will, in the comparisons of this section, only focus our attention on the global norm conservation and the error in the sense of infinite norm while two schemes are implemented. In the last part of this section, we will simulate the global energy transit, which is the change of the discrete global energy as time evolves, for a nonlinear Schrödinger equation by means of the multi-symplectic scheme (33).

We consider the following two problems:

$$\begin{aligned} &\mathrm{i}\psi_t + \alpha_\mu(t)\psi_{xx} + \beta_\mu(t)|\psi|^2\psi = 0,\\ &\psi(x,0) = \varphi_\mu(x), \quad \mu = 1,2, \end{aligned} \tag{65}$$

where

$$\alpha_1(t) = \frac{1}{2}\cos(t), \qquad \beta_1(t) = \frac{\cos(t)}{\sin(t)+3}, \qquad \varphi_1(x) = \frac{1}{\sqrt{3}}\operatorname{sech}\left(\frac{x}{3}\right)\exp\left(\frac{\mathrm{i}(x^2-1)}{6}\right),$$

$$\alpha_2(t) = \frac{1}{2}\left(\cos(t) + \sqrt{2}\cos(\sqrt{2}t)\right), \qquad \beta_2(t) = \frac{\cos(t)+\sqrt{2}\cos(\sqrt{2}t)}{\sin(t)+\sin(\sqrt{2}t)+5},$$

$$\varphi_2(x) = \frac{1}{\sqrt{5}}\operatorname{sech}\left(\frac{x}{5}\right)\exp\left(\frac{\mathrm{i}(x^2-1)}{10}\right).$$

The problem corresponding to $\mu = 1$ is a periodic one, while for $\mu = 2$ it is quasi-periodic. The equation is of interesting and important class of equations (see [43] and references therein). Based on the results in [43], if $\mu = 1$, then the problem has a periodic solitary-wave solution

$$\psi_p(x,t) = P_{1p}(x,t)P_{2p}(x,t)P_{3p}(x,t), \tag{66}$$

where

$$P_{1p}(x,t) = \frac{1}{(\sin(t)+3)^{\frac{1}{2}}},$$

$$P_{2p}(x,t) = \operatorname{sech}\left(\frac{x}{\sin(t)+3}\right),$$

$$P_{3p}(x,t) = \exp\left(\frac{\mathrm{i}(x^2-1)}{2(\sin(t)+3)}\right).$$

If $\mu = 2$, then the problem has a quasi-periodic solitary-wave solution

$$\psi_{qp}(x,t) = P_{1qp}(x,t)P_{2qp}(x,t)P_{3qp}(x,t), \tag{67}$$

where

$$P_{1qp}(x,t) = \frac{1}{(\sin(t)+\sin(\sqrt{2}t)+5)^{\frac{1}{2}}},$$
$$P_{2qp}(x,t) = \operatorname{sech}\left(\frac{x}{\sin(t)+\sin(\sqrt{2}t)+5}\right),$$
$$P_{3qp}(x,t) = \exp\left(\frac{\mathrm{i}(x^2-1)}{2(\sin(t)+\sin(\sqrt{2}t)+5)}\right).$$

In both cases, the uniform grid in both time axis and space axis, with the step size Δt and the step size Δx, respectively, are used.

5.1. Numerical comparisons

Now we take boundary conditions as

$$\psi(-40,t) = \psi(40,t) = 0 \tag{68}$$

and use the mesh

$$x_j = -40 + j\Delta x, \quad j = 1,2,\ldots,n,\ n = \left\lfloor \frac{80}{\Delta x} \right\rfloor,$$
$$t_k = k\Delta t, \quad k = 1,2,\ldots,$$

for our numerical computations.

In each sub-interval, $[t_k, t_{k+1}]$, by using the initial condition in (65) and boundary condition (68), we write (33), (4) and the MG scheme as the form

$$A(k)T(k+1) = B(k)T(k) + F\big(t_k, t_{k+1}, T(k), T(k+1)\big), \quad k = 1,2,\ldots,$$

where $A(k)$ and $B(k)$ are invertible tridiagonal matrices depending on coefficients of the equation, the vector $T(k) = (\psi_{2,k}, \psi_{3,k}, \ldots, \psi_{n-1,k})^{\mathrm{T}}$, and F is the nonlinear term in the nonlinear system determined by the initial condition in (65), boundary condition (68) and coefficients in the equation.

To solve the above nonlinear system, we use the fixed point method. Fixed-point iterations are terminated when both the ∞-norm difference between the $T(k)$s in two successive iterations and the ∞-norm difference between left hand and right hand of the nonlinear system are less than 10^{-14} (the terminating condition).

We denote by

$$e_{\mathrm{sol}} = \max_k (e_{\mathrm{sol}})_k \tag{69}$$

the maximum error with the method under consideration, where $\hat{\psi}$ and ψ are the exact solution and the numerical solution, respectively, and

$$(e_{\mathrm{sol}})_k = \max_j \big|\psi_{j,k} - \hat{\psi}(x_j, t_k)\big|.$$

Table 1
Comparison of the MS scheme (33), the MCN scheme (12) and MG scheme for the periodic problem (63) ($\mu = 1$)

$\Delta t \backslash \Delta x$	$\Delta x = 0.2$				
	mthd	N	It	e_{sol}	e_{unit}
$\Delta t = 0.4$	MS	439	50	3.5236×10^{-2}	7.5495×10^{-15}
	MCN	440	50	4.5316×10^{-2}	1.3636×10^{-13}
	MG	39	50	4.5314×10^{-2}	1.5166×10^{-13}
$\Delta t = 0.2$	MS	361	50	1.1486×10^{-2}	4.8850×10^{-15}
	MCN	361	50	2.5283×10^{-2}	4.5075×10^{-14}
	MG	362	50	2.5283×10^{-2}	2.0206×10^{-14}
$\Delta t \backslash \Delta x$	$\Delta x = 0.4$				
$\Delta t = 0.4$	MS	438	50	2.8661×10^{-2}	8.6597×10^{-15}
	MCN	438	50	5.6458×10^{-2}	1.5810×10^{-13}
	MG	439	50	5.6454×10^{-2}	1.4522×10^{-13}
$\Delta t = 0.2$	MS	362	50	6.6728×10^{-2}	4.6629×10^{-15}
	MCN	363	50	4.2482×10^{-2}	1.7764×10^{-14}
	MG	362	50	4.2479×10^{-2}	1.8208×10^{-14}
$\Delta t \backslash \Delta x$	$\Delta x = 0.4$				
$\Delta t = 0.4$	MS	877	100	2.8808×10^{-2}	1.1546×10^{-14}
	MCN	876	100	5.6516×10^{-2}	3.2041×10^{-13}
	MG	878	100	5.6511×10^{-2}	2.8377×10^{-13}
$\Delta t = 0.2$	MS	1492	200	6.7160×10^{-2}	7.1054×10^{-15}
	MCN	1492	200	4.2610×10^{-2}	4.4853×10^{-14}
	MG	1490	200	4.2608×10^{-2}	4.3299×10^{-14}

The symbols are as follows: 'mthd' stands for method, 'N' is the number of fixed point iterations, 'It' is the total number of time steps, 'e_{sol}' is given by (69), while 'e_{unit}' is the unitarity error given by (38) for MS and (53) for MCN. See text for details.

The multi-symplectic scheme (33) (in short, **MS**), the modified Cranck–Nicolson scheme (12) (in short, **MCN**) and the MG scheme, have been run on the same machine for the two problems $\mu = 1, 2$.[1] The result of our computations is displayed in Tables 1 and 2.

In the last column of each table we display the error on the conservation laws (38) for MS and (53) for MCN. The errors are computed as

$$e_{\text{unit}} = \max_k \left| \|\psi_k\|_{\frac{1}{2}}^2 - \|\hat{\psi}_k\|_{\frac{1}{2}}^2 \right| \tag{70}$$

for the MS scheme, and

$$e_{\text{unit}} = \max_k \left| \|\psi_k\|^2 - \|\hat{\psi}_k\|^2 \right| \tag{71}$$

for the MCN scheme and the MG scheme.

For the periodic problem, the numerical simulations reveal that all methods preserve well their discrete conservation laws (38) and (53) which is possessed by MG scheme, the error being essentially determined by the tolerance on fixed-point iterations. Furthermore, it is evident that the numerical behavior of the

[1] Note that all methods are implicit and all obey discrete conservation laws.

Table 2
Comparison of the MS scheme (33), the MCN scheme (12) and the MG scheme for the quasi-periodic problem (63) ($\mu = 2$)

$\Delta t \backslash \Delta x$	$\Delta x = 0.2$				
	mthd	N	It	e_{sol}	e_{unit}
$\Delta t = 0.4$	MS	390	50	1.0027×10^{-1}	9.3259×10^{-15}
	MCN	389	50	1.0674×10^{-1}	7.7983×10^{-14}
	MG	389	50	1.0673×10^{-1}	8.1046×10^{-14}
$\Delta t = 0.2$	MS	310	50	5.1756×10^{-2}	9.7700×10^{-15}
	MCN	311	50	6.1279×10^{-2}	4.2188×10^{-14}
	MG	311	50	6.1277×10^{-2}	4.2633×10^{-14}
$\Delta t \backslash \Delta x$	$\Delta x = 0.4$				
$\Delta t = 0.4$	MS	389	50	8.9485×10^{-2}	2.8866×10^{-15}
	MCN	389	50	1.1338×10^{-1}	8.1046×10^{-14}
	MG	389	50	1.1337×10^{-1}	8.3267×10^{-14}
$\Delta t = 0.2$	MS	311	50	3.9445×10^{-2}	3.3307×10^{-15}
	MCN	311	50	7.2450×10^{-2}	4.0412×10^{-14}
	MG	311	50	7.2447×10^{-2}	4.1522×10^{-14}
$\Delta t \backslash \Delta x$	$\Delta x = 0.4$				
$\Delta t = 0.4$	MS	770	100	9.1156×10^{-2}	4.2188×10^{-15}
	MCN	769	100	1.2034×10^{-1}	1.2323×10^{-13}
	MG	769	100	1.20337×10^{-1}	1.2412×10^{-13}
$\Delta t = 0.2$	MS	1315	200	5.2132×10^{-2}	1.0214×10^{-14}
	MCN	1315	200	8.5937×10^{-2}	1.1124×10^{-13}
	MG	1315	200	8.5926×10^{-2}	1.1724×10^{-13}

The symbols are as in Table 1.

MS scheme is, in general, better than MCN and MG. While $\Delta t = 0.2$ and $\Delta x = 0.4$, data tell us that the average error, in some sense, of MS scheme seems less than MCN and MG. The appearance of this case implies that the implementation of MS (also (4)) is partly depending on the ratio $\frac{\Delta t}{\Delta x}$ (of course, on the terminating condition and so on) (see [20]).

For the quasi-periodic problem, all cases for Δt and Δx, the numerical behavior of the MS scheme is better than MCN and MG, and the discrete conservation laws (38) and (53) are preserved to an accuracy of between 10^{-15} and 10^{-13}.

Numerical results in both two tables do not, in evidence, reveal the superiority of the multi-symplectic scheme (33) over two others. Now we take the computational time interval $[0, 120]$, which is longer than in the tables, and let $\Delta t = 0.4$ and $\Delta x = 0.4$. The boundary condition is taken as (68). The terminating condition of fixed point iteration is the same as the above.

Figs. 1–3 show that the variation of $(e_{\text{sol}})_k$ of MS, MCN and MG, respectively, in the periodic case. Errors in all figures oscillate in the almost periodic state. Comparing with the corresponding cases in Table 1 (in the time interval $[0, 40]$), e_{sol} in the time interval $[0, 200]$ does not change in the sense of roundoff. This accords with the result in Section 4.

Figs. 4–6 show that the variation of the error $(e_{\text{unit}})_k$ of MS, MCN and MG, respectively, in the periodic case. The first interesting observation, looking at the error curves in the figures, is that the trends of errors are increasing when t becomes larger. The second interesting observation is that in the sense of

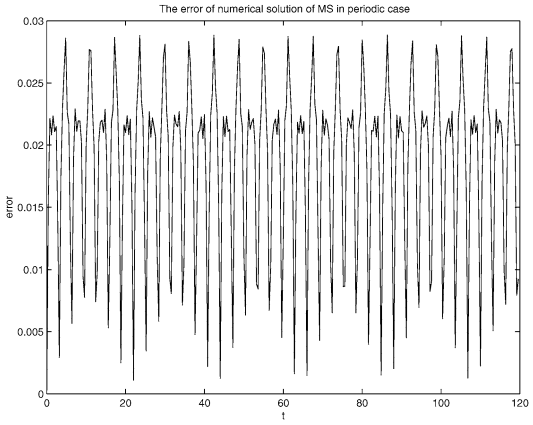

Fig. 1. The variation of $(e_{\mathrm{sol}})_k$ of MS, where $\Delta t = \Delta x = 0.4$, and $e_{\mathrm{sol}} = 0.02885269331356$.

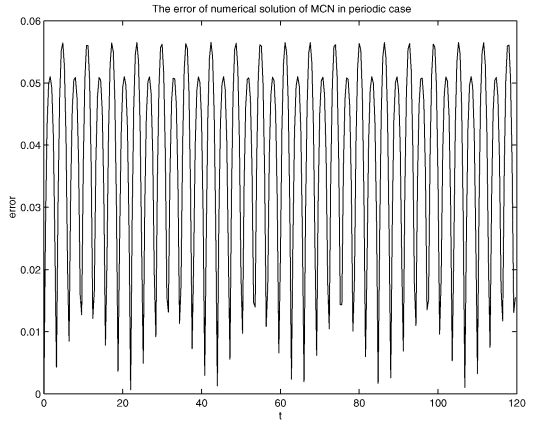

Fig. 2. The variation of $(e_{\mathrm{sol}})_k$ of MCN, where $\Delta t = \Delta x = 0.4$, and $e_{\mathrm{sol}} = 0.05653228435476$.

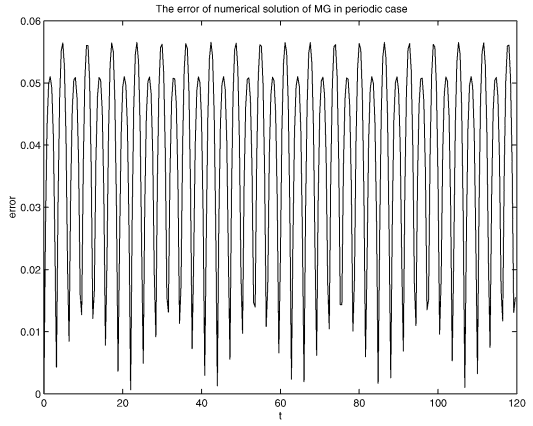

Fig. 3. The variation of $(e_{\mathrm{sol}})_k$ of MG, $\Delta t = \Delta x = 0.4$, and $e_{\mathrm{sol}} = 0.05652822484364$.

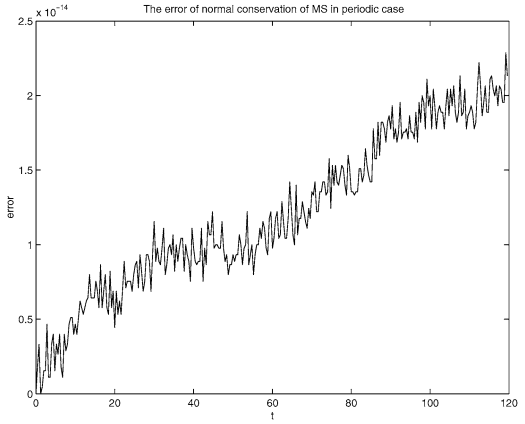

Fig. 4. The variation of $(e_{\text{unit}})_k$ of MS, where $\Delta t = \Delta x = 0.4$, and $e_{\text{unit}} = 2.287059430727823\text{e–}014$, $(e_{\text{unit}})_k = |\|\psi_k\|_{\frac{1}{2}}^2 - \|\hat{\psi}_k\|_{\frac{1}{2}}^2|$.

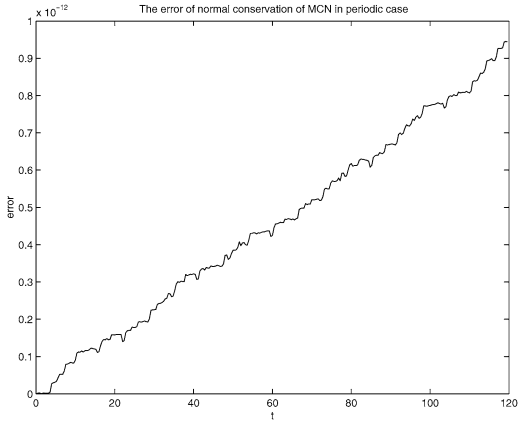

Fig. 5. The variation of $(e_{\text{unit}})_k$ of MCN, where $\Delta t = \Delta x = 0.4$, and $e_{\text{unit}} = 9.450218385609333\text{e–}013$, $(e_{\text{unit}})_k = |r\|\psi_k\|^2 - \|\hat{\psi}_k\|^2|$.

corresponding discretizations, the increasing rate of error of MS scheme is obviously less that others. In fact, from Table 1 and figures, it is follows that the maximum error e_{unit} of MS increases about 1.1324×10^{-14} from $t = 40$ to $t = 120$, but the maximum errors of MCN and MG increase about 6.2459×10^{-13} and 4.8603×10^{-13}, respectively, in the same time interval. These numerical phenomena seems to infer that *the multi-symplectic scheme* (33) *has a better numerical stability in discrete norm conservation.*

Figs. 7–9 show that the variation of $(e_{\text{sol}})_k$ of MS, MCN and MG, respectively, in the quasi-periodic case. For all three numerical schemes, e_{sol} for the time interval $[0, 120]$ is not different from one for $[0, 40]$ in Table 2.

Figs. 10–12 show that the variation of $(e_{\text{unit}})_k$ of MS, MCN and MG, respectively, in the quasi-periodic case. Fig. 10 tells us that e_{unit} does not change in the interval $[0, 95]$ in the sense of roundoff, at about $t = 96$, it suddenly jumps to a little higher magnitude, and increases about 5.7732×10^{-15}. For MCN

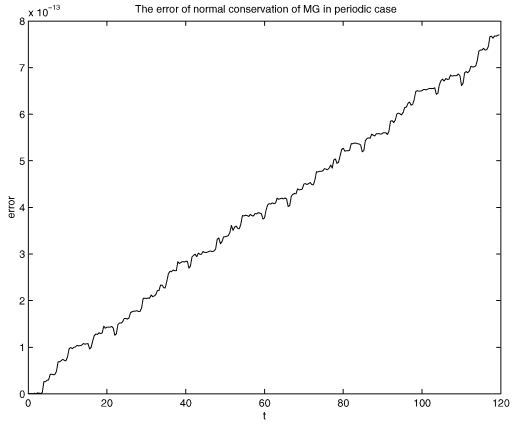

Fig. 6. The variation of $(e_{\text{unit}})_k$ of MG, where $\Delta t = \Delta x = 0.4$, and $e_{\text{unit}} = 7.698286452750836\text{e–}013$, $(e_{\text{unit}})_k = |\|\psi_k\|^2 - \|\hat{\psi}_k\|^2|$.

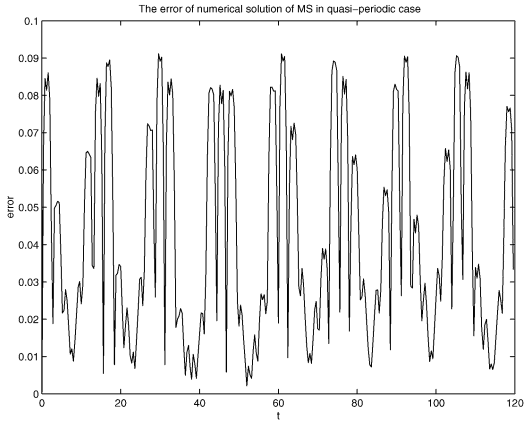

Fig. 7. The variation of $(e_{\text{sol}})_k$ of MS, where $\Delta t = \Delta x = 0.4$, and $e_{\text{sol}} = 0.09115641996455$.

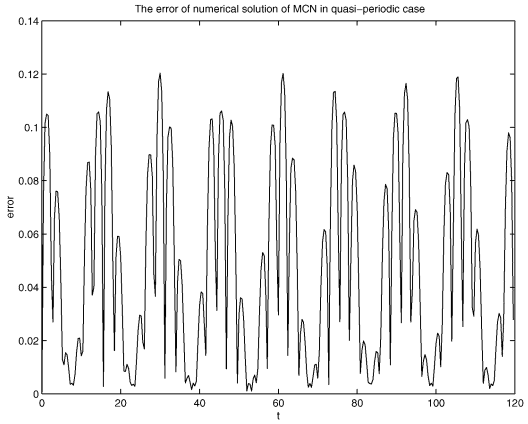

Fig. 8. The variation of $(e_{\text{sol}})_k$ of MCN, where $\Delta t = \Delta x = 0.4$, and $e_{\text{sol}} = 0.12034447457798$.

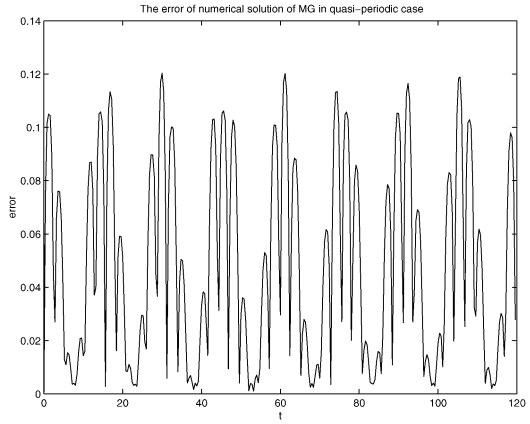

Fig. 9. The variation of $(e_{\text{sol}})_k$ of MG, where $\Delta t = \Delta x = 0.4$, and $e_{\text{sol}} = 0.12033695254764$.

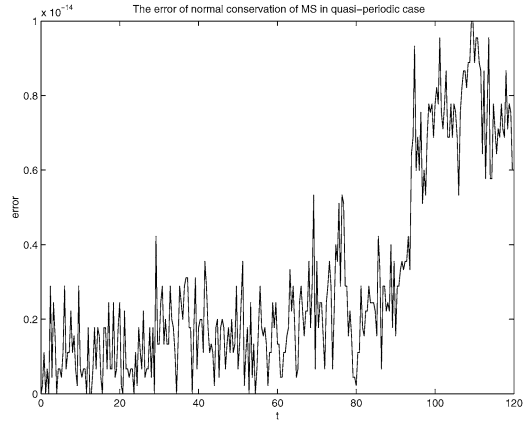

Fig. 10. The variation of $(e_{\text{unit}})_k$ of MS, where $\Delta t = \Delta x = 0.4$, and $e_{\text{unit}} = 9.992007221626409\text{e–}015$, $(e_{\text{unit}})_k = |\|\psi_k\|_{\frac{1}{2}}^2 - \|\hat{\psi}_k\|_{\frac{1}{2}}^2|$.

and MG, numerical results in Figs. 11, 12 and Table 2 show that the maximum errors e_{unit} increase 3.4151×10^{-13} and 2.969×10^{-13}, respectively.

A very interesting observation, looking at Tables 1, 2 and figures, is that the numerical efficiency and behavior of the scheme MG are the same as the scheme MCN.

In Figs. 13 and 14, the periodically solitary wave and quasi-periodic solitary wave are pictured numerically with $\Delta t = 0.4$ and $\Delta x = 0.4$.

5.2. *Energy transit of the multi-symplectic scheme*

Now we consider the energy transit of the multi-symplectic scheme. The problem (65) does not have the property of global energy conservation because its nonlinear term is explicitly depending on the time t. In order to monitor the discrete global energy transit of (33), we consider the problem

$$\mathrm{i}\psi_t + \psi_{xx} + |\psi|^2\psi = 0, \qquad \psi(x,0) = \varphi(x), \tag{72}$$

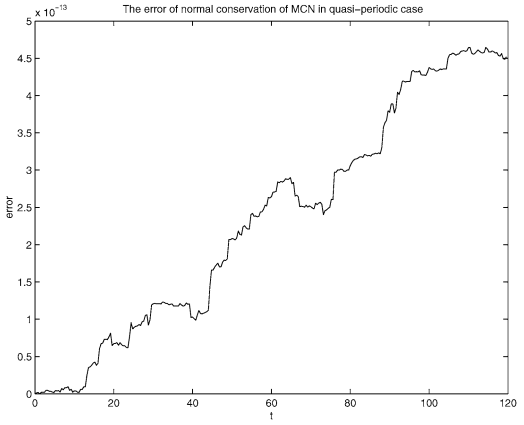

Fig. 11. The variation of $(e_{\text{unit}})_k$ of MCN, where $\Delta t = \Delta x = 0.4$, and $e_{\text{unit}} = 4.647393581080905\text{e–}013$, $(e_{\text{unit}})_k = |\|\psi_k\|^2 - \|\hat{\psi}_k\|^2|$.

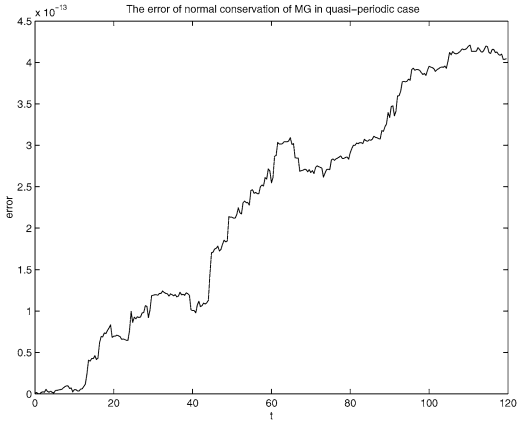

Fig. 12. The variation of $(e_{\text{unit}})_k$ of MG, where $\Delta t = \Delta x = 0.4$, and $e_{\text{unit}} = 4.209965709378594\text{e–}013$, $(e_{\text{unit}})_k = |\|\psi_k\|^2 - \|\hat{\psi}_k\|^2|$.

where

$$\varphi(x) = \frac{\sqrt{2}}{2}\exp\left(\mathrm{i}\frac{x}{2}\right)\operatorname{sech}\left(\frac{x}{2}\right).$$

By using (33) with $\alpha \equiv 1$, and $\beta \equiv 1$, and a periodic boundary condition, the discrete global energy is

$$E(t_k) = \Delta x \sum_j \left(\left| \frac{\psi_{j+1,k} - \psi_{j,k}}{\Delta x} \right|^2 - \frac{1}{2} \left| \frac{\psi_{j+1,k} + \psi_{j,k}}{2} \right|^4 \right), \tag{73}$$

with $t_0 = 0$. We take the periodic boundary condition

$$\psi(-20, t) = \psi(20, t) = 0,$$

and $\Delta t = 0.05$, $\Delta x = 0.2$, and simulate numerically $E(k)$, for $k = 1, \ldots, 200$, in terms of the method in Section 5.1 with the terminating condition 10^{-12}. The result of our computation is

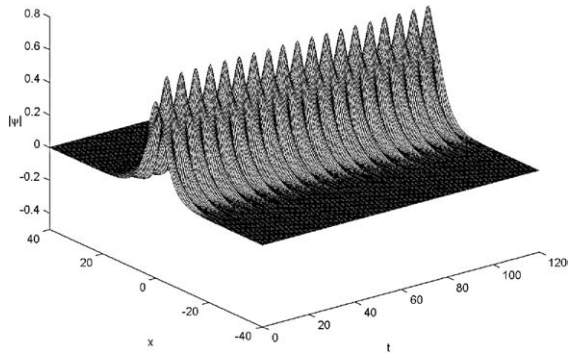

Fig. 13. The periodically solitary wave of (65) in the case $\mu = 1$ with $\Delta t = 0.4$ and $\Delta x = 0.4$.

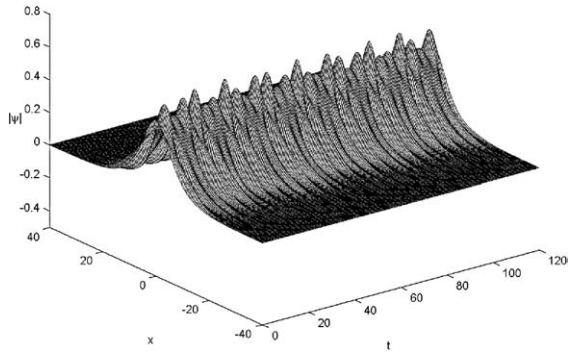

Fig. 14. The quasi-periodic solitary wave of (65) in the case $\mu = 2$ with $\Delta t = 0.4$ and $\Delta x = 0.4$.

$$E_{\max} = \max_{0\leqslant k\leqslant 200} E(t_k) = 3.345461352208954 \times 10^{-1};$$

$$E_{\min} = \min_{0\leqslant k\leqslant 200} E(t_k) = 3.345457472328555 \times 10^{-1};$$

$$E_{\text{error}} = \max_{0\leqslant k\leqslant 200} \left|E(t_k) - E(t_0)\right| = 3.87988 \times 10^{-7}.$$

Fig. 15 exhibits the conservation of global energy, and shows the curve of global energy in the sense of translation (here we picture $E(t_k) - 0.3345459$). The curve viewed in Fig. 15 reveals that the discrete global energy is lost in a small scale ($\approx 10^{-5}$), with the time evolution under the multi-symplectic scheme (33). Note that

$$e_{\text{sol}} = 3.8617 \times 10^{-2}.$$

In contrast of the accuracy of the scheme (33), the discrete global energy is preserved very well, while the discrete norm is preserved with

$$e_{\text{unit}} = 2.0006 \times 10^{-13}.$$

Finally, we take $\Delta t = 0.2$ and $\Delta x = 0.2$, and implement MS for $0 \leqslant k \leqslant 1000$ and the same boundary condition and terminating condition as the above. Fig. 16, in the sense of translation ($E(t_k) - 0.3345459$ is pictured), provides the discrete global energy and the change of global energy transit in small scale

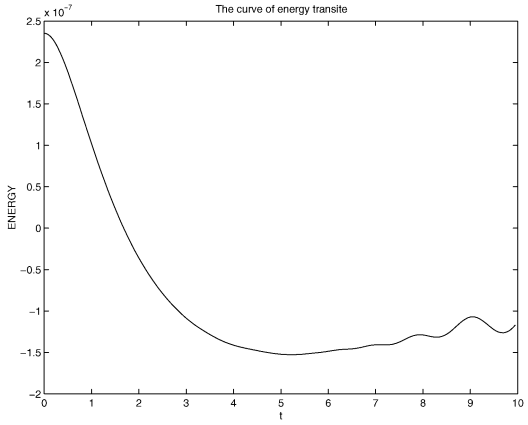

Fig. 15. The curve of global energy transit is pictured in terms of $E(t_k) - 0.3345459$.

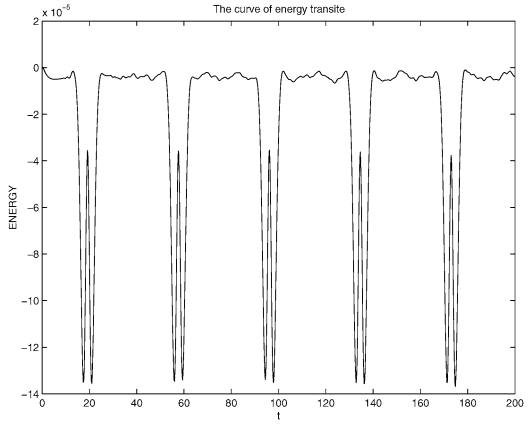

Fig. 16. The curve of global energy transit with $\Delta t = 0.2$ and $\Delta x = 0.2$ and $0 \leqslant k \leqslant 1000$.

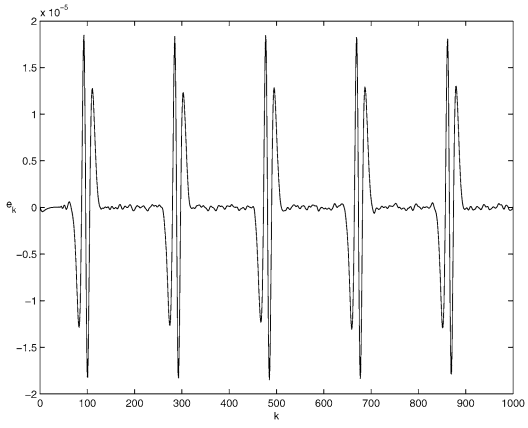

Fig. 17. e_k in Corollary 1 in Section 3 with $\Delta t = 0.2$ and $\Delta x = 0.2$ and $0 \leqslant k \leqslant 1000$.

($\approx 10^{-5}$). Fig. 17 is for e_k in Corollary 1 in Section 3. In this case, e_{sol} has been crazy (≈ 1.8493)! However, the discrete global energy still has very nice numerical behavior, the result of our computation is

$$e_{\text{unit}} = 9.319656 \times 10^{-12};$$
$$E_{\max} = \max_{0 \leqslant k \leqslant 1000} E(t_k) = 3.345461352208994 \times 10^{-1};$$
$$E_{\min} = \min_{0 \leqslant k \leqslant 1000} E(t_k) = 3.3440907112219 \times 10^{-1};$$
$$E_{\text{error}} = \max_{0 \leqslant k \leqslant 1000} \left| E(t_k) - E(t_0) \right| = 1.370645 \times 10^{-4};$$
$$\max_{0 \leqslant k \leqslant 1000} \mathrm{e}_k = 1.8493 \times 10^{-5}.$$

6. Conclusion

In conclusion, for Schrödinger equations with varying coefficients, the multi-symplectic scheme considered in this paper is proved to preserve exactly the norm conservation and to be stable and convergent with respect to the initial values. In comparison with a nice conservative scheme (MCN) and another multi-symplectic scheme (MG), the multi-symplectic scheme (MS) is slightly (somewhat) ascendant in the preservation of discrete norm conservation, thus in the corresponding stability (in the sense of norm conservation law) in long time computation. Although MS does not preserve theoretically the global energy, the numerical accuracy of global energy, in numerical simulation of the last part 5.2 of paper for the case of constant coefficients, can arrive at a higher order in contrast of the accuracy of numerical solutions of the multi-symplectic scheme (MS). Our numerical results match theoretical ones in this paper.

References

[1] M.J. Ablowitz, C.M. Schober, Hamiltonian integrators for the nonlinear Schrödinger equation, Internat. J. Modern Phys. C 5 (1994) 397–401.
[2] S. Blanes, P.C. Moan, Splitting methods for the time-dependent Schrödinger equation, Phys. Lett. A 265 (2000) 35–42.
[3] J. Bourgain, Global Solutions of Nonlinear Schrödinger Equations, Amer. Math. Soc. Colloq. Publ., vol. 46, American Mathematical Society, Providence, RI, 1999.
[4] T.J. Bridges, Multi-symplectic structures and wave propagation, Math. Proc. Cambridge Philos. Soc. 121 (1997) 147–190.
[5] T.J. Bridges, S. Reich, Multi-symplectic integrators: numerical schemes for Hamiltonian PDEs that conserve symplecticity, Phys. Lett. A 284 (4–5) (2001) 184–193.
[6] C.J. Budd, M.D. Piggott, Geometric integration and its application, in: Handbook Numer. Anal., vol. XI, North-Holland, Amsterdam, 2003, pp. 35–139.
[7] J. Chen, M-Z. Qin, Multi-symplectic geometry and multisymplectic integrators for the nonlinear Schrödinger equation, Preprint, 2000.
[8] J. Chen, New schemes for the nonlinear Schrödinger equation, Appl. Math. Comput. 124 (2001) 371–379.
[9] M. Delfour, M. Fortin, G. Payre, Finite-difference solutions of a non-linear Schrödinger equation, J. Comput. Phys. 44 (1981) 277–288.
[10] K. Feng, Collected Works of Feng Kang II, National Defence Industry Press, Beijing, 1995.
[11] I. Galbraith, Y.S. Ching, E. Abraham, Two-dimensional time-dependent quantum-mechanical scattering event, Amer. J. Phys. 52 (1) (1984) 60–68.

[12] S.K. Gray, D.E. Manolopoulos, Symplectic integrators tailored to the time-dependent Schrödinger equation, J. Chem. Phys. 104 (18) (1996) 7099–7112.
[13] A. Goldberg, H.M. Schey, Computer-generated motion pictures of one-dimensional quantum-mechanical transmission and reflection phenomena, Amer. J. Phys. 35 (3) (1967) 177–186.
[14] B.M. Herbst, J. Morris, A.R. Mitchell, Numerical experiment with the nonlinear Schrödinger equation, J. Comput. Phys. 60 (1985) 282–305.
[15] B.M. Herbst, F. Varadi, M.J. Ablowitz, Symplectic methods for the nonlinear Schrödinger equation, Math. Comput. Simulation 37 (1994) 353–369.
[16] J. Hong, Y. Liu, Multi-symplecticity of the centred box discretizations for a class of Hamiltonian PDE's and an application to quasi-periodically solitary wave of qpKdV equation, Math. Comput. Model. 39 (2004) 1035–1047.
[17] J. Hong, Y. Liu, A novel numerical approach to simulating nonlinear Schrödinger equation with varying coefficients, Appl. Math. Lett. 16 (2003) 759–765.
[18] J. Hong, M.-Z. Qin, Multi-symplecticity of the centred box discretizations for Hamiltonian PDE's with $m \geqslant 2$ space dimensions, Appl. Math. Lett. 15 (2002) 1005–1011.
[19] X.-G. Hu, Laguerre Scheme: Another member for propagating the time-dependent Schrödinger equation, Phys. Rev. E 59 (2) (1999) 2471–2474.
[20] A. Iserles, A First Course in the Numerical Analysis of Differential Equations, Cambridge University Press, Cambridge, 1996.
[21] A.L. Islas, D.A. Karpeev, C.M. Schober, Geometric integrations for the nonlinear Schrödinger equation, J. Comput. Phys. 173 (2001) 116–148.
[22] S. Jiménez, L. Vázquez, Some remarks on conservative and symplectic schemes, in: Nonlinear Problems in Future Particle Accelerators, Proceedings, World Scientific, Singapore, 1991, pp. 151–162.
[23] S. Jiménez, Derivation of the discrete conservation laws for a family of finite difference schemes, Appl. Math. Comput. 64 (1994) 13–45.
[24] D.A. Karpeer, C.M. Schober, Symplectic integrators for discrete nonlinear Schrödinger systems, Math. Comput. Simulation 56 (2001) 145–156.
[25] H.J. Korsch, H. Wiescher, Quantum chaos, in: K.H. Hoffmann, M. Schreiber (Eds.), Computational Physics, Springer, Berlin, 1996, pp. 225–244.
[26] L.D. Landau, M.E. Lifshitz, Quantum Mechanics, Non-Relativistic Theory, Pergamon, London, 1977.
[27] T.D. Lee, Difference equations and conservation laws, J. Statist. Phys. 46 (5/6) (1987) 843–860.
[28] S. Li, L. Vu-Quoc, Finite difference calculus invariant structure of a class of algorithms for the nonlinear Klein–Gordon equation, SIAM J. Numer. Anal. 32 (6) (1995) 1839–1875.
[29] J.E. Marsden, G.P. Patrick, S. Shkoller, Multisymplectic geometry, variational integrators, and nonlinear PDEs, Comm. Math. Phys. 199 (1998) 351–395.
[30] J.E. Marsden, S. Pekarsky, S. Shkoller, M. West, Variational methods, multisymplectic geometry and continuum mechanics, J. Geom. Phys. 38 (2001) 253–284.
[31] J.E. Marsden, S. Shkoller, Multisymplectic geometry, covariant Hamiltonians and water waves, Math. Proc. Cambridge Philos. Soc. 125 (1999) 553–575.
[32] R.I. McLachlan, S.K. Gray, Optimal stability polynomials for splitting methods, with application to the time-dependent Schrödinger equation, Appl. Numer. Math. 25 (1997) 275–286.
[33] R.M. Neal, An improved acceptance procedure for the hybrid Monte Carlo algorithm, J. Comput. Phys. 111 (1994) 194–203.
[34] I.V. Puzyin, A.V. Selin, S.I. Vinitsky, A high-order accuracy method for numerical solving of the time-dependent Schrödinger equation, Comput. Phys. Comm. 123 (1999) 1–6.
[35] I.V. Puzyin, A.V. Selin, S.I. Vinitsky, Magnus-factorized method for numerical solving the time-dependent Schrödinger equation, Comput. Phys. Comm. 126 (2000) 158–161.
[36] J.I. Ramos, Linearly implicit methods for the nonlinear Schrödinger equation in nonhomogeneous media, Appl. Math. Comput. 133 (2002) 1–28.
[37] S. Reich, Multi-symplectic Runge–Kutta methods for Hamiltonian wave equations, J. Comput. Phys. 157 (2000) 473–499.
[38] J.M. Sanz-Serna, M.P. Calvo, Numerical Hamiltonian Problems, Chapman and Hall, London, 1994.
[39] J.M. Sanz-Serna, J.G. Verwer, Conservative and nonconservative schemes for the solution of the nonlinear Schrödinger equation, IMA J. Numer. Anal. 6 (1986) 25–42.

[40] J.M. Sanz-Serna, Methods for numerical solution of the nonlinear Schrödinger equation, Math. Comp. 43 (1984) 21–27.
[41] J.M. Sanz-Serna, V.S. Manoranjan, A method for the integration in time of certain partial differential equations, J. Comput. Phys. 52 (1983) 273–289.
[42] C.M. Schober, Symplectic integrators for the Ablowitz–Ladik discrete nonlinear Schrödinger equation, Phys. Lett. A 259 (1999) 140–151.
[43] V.N. Serkin, A. Hasegawa, Novel soliton solutions of the nonlinear Schrödinger equation model, Phys. Rev. Lett. 85 (21) (2000) 4502–4505.
[44] C. Sulem, P.-L. Sulem, The Nonlinear Schrödinger Equation, Self-Focusing and Wave Collapse, Springer, New York, 1999.
[45] F. Zhang, V.M. Pérez-García, L. Vázquez, Numerical simulation of nonlinear Schrödinger systems: A new conservative scheme, Appl. Math. Comput. 71 (1995) 165–177.